Master's thesis

Ligand Mediated Surface Reconstruction of Photoluminescent CdTe Quantum Dots

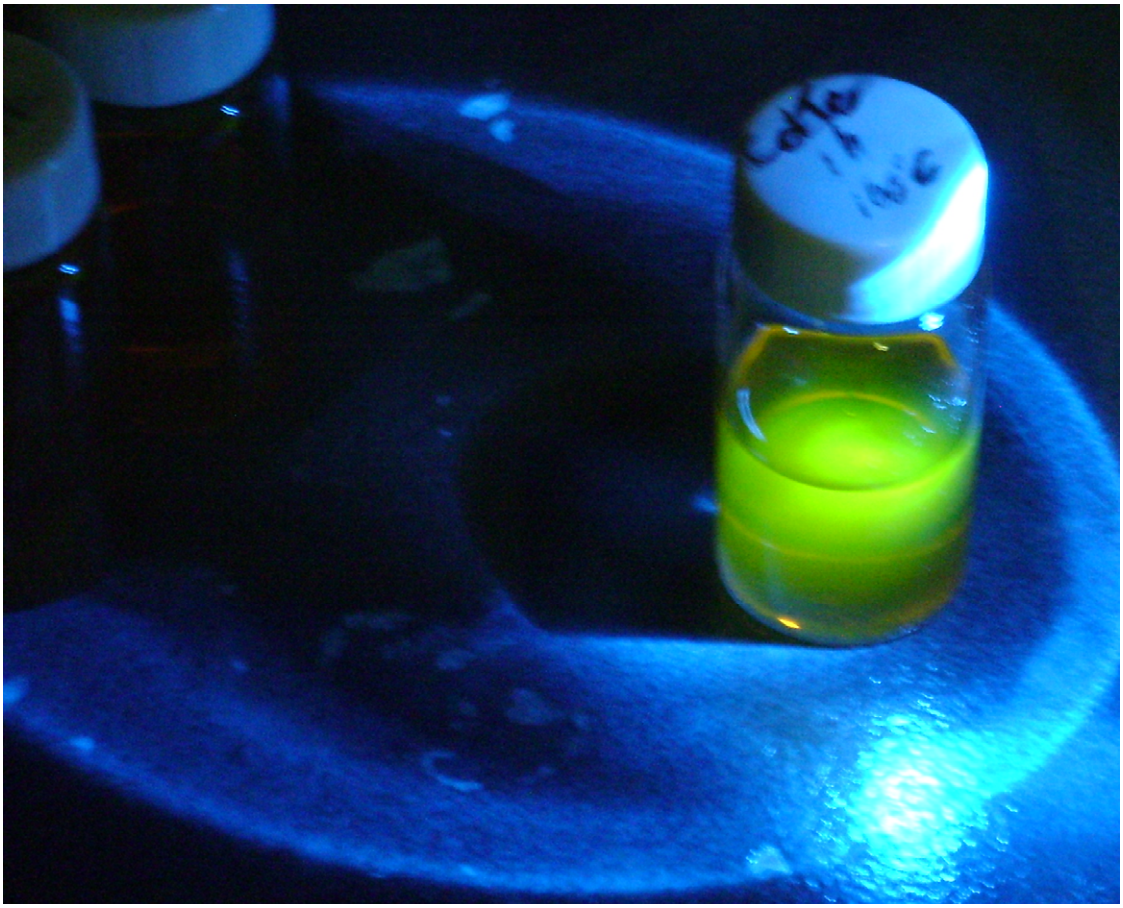

Arnoud Onnink

Supervisors:

Esther Groeneveld
Celso de Mello Donegá

Condensed Matter and Interfaces
Debye Institute for Nanomaterials Science
Utrecht University

6 July 2012

Abstract

Enhancement of photoluminescence (PL) is observed for light-shielded dodecylamine-capped colloidal CdTe quantum dots (CdTe/DDA QDs) dispersed in toluene after washing and recapping. The PL quantum yield (QY) increases from 19% to 25% in 25 hours, indicating gradual reconstruction of the surface. This enhancement is contrasted with PL quenching of light-shielded CdTe QDs recapped with octadecylamine (CdTe/ODA), for which the QY decreases from 17% to 15% in 26 hours. The differences in PL evolution are explained by the presence of ligand-imposed energy barriers on the order of kT and > kT for surface reconstruction of the DDA- and ODA-capped surfaces, respectively. This is supported by the observation of enhancement of the PL QY from 19% to 27% in 26 hours for CdTe/DDA and 17% to 21% for CdTe/ODA QDs that are exposed to short flashes of 400 nm light. The kinetics are related to interactions between amine alkyl chains by vibrational spectroscopy. The results demonstrate the active involvement of the amine capping layer in NC surface reconstruction. A model is proposed that explains this form of surface reconstruction as a transition from a state in which the rigid capping layer imposes disorder on the NC, to a state in which the NC dictates the configuration of the capping layer. It is suggested that illumination locally heats the capping layer of QDs in which the exciton decays non-radiatively, so that the effect is similar to earlier reports of luminescence temperature antiquenching in amine-capped CdSe QDs.

Contents

1 Introduction

Classical high school chemistry teaches that every chemical compound has a fixed set of intensive properties[1] that can be used to distinguish it from other compounds. For example a soft, metallic yellow solid that conducts well and melts at 1337 K is easily identified as elemental gold. However, as with all such concepts in science, this ideal view is only valid under certain conditions. While high school science only mentions temperature, pressure and perhaps polymorphism as factors of influence, modern science has given increasing attention to another variable that can have major effects on the properties of a material: size.

The notion that size matters lies at the foundation of the modern interdisciplinary field of nanoscience. Materials of interest to this field are referred to as nanoscopic materials or nanomaterials because their atoms are arranged in structures with sizes smaller than 100 nm in at least one of the three spatial dimensions. This gives rise to remarkable properties: for example, gold nanocrystals (NCs) may have a melting point as low as 800 K [1] and their colour ranges between red, purple and blue depending on their dimensions [2]. A small gold coin and a large gold bar will both have the same yellow colour and melt at 1337 K: for the properties of such macroscopic or bulk materials, size does not matter and the classical view on intensive properties applies accordingly.

Many different nanomaterials have been made from a wide variety of compounds besides gold, each with its own properties and potential applications. A particular type is the quantum dot (QD), a NC of a semiconductor compound such as cadmium selenide (CdSe) or cadmium telluride (CdTe). QDs have attracted increasing interest due to their photoluminescence (PL): the absorption and subsequent emission of light. Whereas bulk crystals of CdTe and CdSe appear black to the human eye due to their absorption of visible light and emission in the infrared, NCs of these II-VI semiconductors absorb and emit visible light of a colour depending on the crystal size. This is illustrated by figure 1.1 below. In the next chapter a quantum mechanical explanation is given for the optical properties of such NCs, which are called dots because they are smaller than 100 nm in all three dimensions.

Certain types of nanomaterials were already produced back in the days of alchemy, although their nanoscopic nature was not recognized until the 20th century. For example the 17th century alchemist Andreas Cassius described the preparation of a dye with a tunable purple colour using gold in his treatise *De auro*, that was later found to consist of the aforementioned gold NCs. With the advent of nanoscience many other types of nanomaterials have been reported, with potential applications ranging from the cooling of computer chips with nanoheatsinks [3] to water purification. [4] However, many of these applications require further research before they can be realized. A particular issue addressed in this thesis is the stability of the properties of NCs.

Figure 1.1: *Colloidal CdSe QDs of increasing size from left to right, showing a change in emission colour. The dots were excited by illumination with UV-light. Image courtesy of M. Vis (Utrecht University).*

[1] In the macroscopic view of physical chemistry, intensive properties of a system are independent of its size. This is opposed to extensive properties such as mass, which depend on the system size even in the macroscopic limit. On the nanoscale some properties that are commonly considered intensive become extensive, such as the melting point.

QDs are a promising type of modern nanomaterials. The first understanding of their synthesis and properties in relation to their size emerged in the early 1980s [5] and research has since shown that they have a wide variety of potential applications due to their optical and electrical properties. Solar cells, for example, may benefit from using QDs as sensitizers that absorb sunlight, a function that is currently often performed by silicon or organic dyes. Other applications for which QDs have attracted interest because of their well-defined and tunable emission are light emitting diodes (LEDs), QD lasers and targeted biological imaging. [6]

Macroscopic amounts of QDs can be conveniently produced by growing them in a solution of coordinating surfactants. The resulting colloids are essentially inorganic-organic hybrid nanomaterials, consisting of an inorganic NC with an organic ligand coating. The surfactants are not only essential to preventing aggregation of the colloidal NCs, but also influence their properties by changing the electronic structure and free energy landscape of the inorganic surface that they bind to. In this way, much of the identity of a QD is determined at the surface-ligand interface, as its nanoscopic nature entails that a large fraction of its atoms resides there.

Indeed, experiments show that the PL of QDs is strongly influenced by the type [7], amount [8] and distribution [9] of ligands on the crystal surface. For example, in my bachelor's thesis I reported how replacing the dodecylamine (DDA) cap of colloidal CdTe QDs with hexanethiol (HT) can lead to both an increase or decrease in the PL intensity, depending on the amount of thiols added. At the optimal concentration, thiol ligands effectively passivate electron traps in the crystal [10], which has been observed to double PL intensities in some samples.

Whereas thiol ligands enhance the PL of a colloidal CdTe QD by directly changing its electronic structure, amine ligands on CdSe have been reported to do so indirectly by allowing the NC surface to reconstruct above a certain temperature. This effect was dubbed luminescence temperature anti-quenching (LTAQ) because PL was found to be enhanced with increasing temperature, rather than quenched as normally expected. [11] LTAQ and similar effects demonstrate that the influence of the capping layer on the properties of QDs can be directed with methods less invasive than chemical exchange procedures, such as heating or illumination. [12]

This thesis documents enhancement of the PL in colloidal DDA-capped CdTe QDs that are not exposed to new surfactants, heated above room temperature or illuminated. The effect was captured by following the evolution of the PL over several hours, starting at the moment the QDs are dispersed in toluene. For a typical sample, the quantum yield increased from 19% to 25% after 9 hours. The effect of illumination on these CdTe QD dispersions was also investigated, including how it influenced the enhancement of the various samples.

In addition to optical spectroscopy inside a glovebox, several techniques were employed to test whether frequently stated hypotheses on the mechanisms behind PL enhancement could account for the reported results. Dynamic light scattering (DLS) was used to track the hydrodynamic radius of the colloidal NCs as a function of time. PL measurements were repeated with CdTe QDs covered by longer ODA surfactants, to determine the effect of the alkyl chain length on the evolution of the PL. The role of the surfactant layer was further investigated by following the infrared absorption at vibrational energies specific to bound and unbound amine ligands.

The results are used to construct a model that paints a lively picture of the dance between a NC and its ligands. In this way, the model sheds new light on the processes that shape the identity of the crystal. Such knowledge is hoped to assist in the quest for functionalization and optimization of colloidal QDs, so that these tiny crystals can fulfill their great potential for the tasks they are envisioned to perform in the coming decade.

2 Theory

As a result of their nanometer dimensions, semiconductor nanocrystals (NCs) or quantum dots (QDs) show remarkably different properties compared to their bulk counterparts. These properties depend strongly on the size of the inorganic crystals. For example, the photoluminescence of QDs shifts to shorter wavelengths as the crystal size decreases, as illustrated by figure 1.1. As this thesis focuses on solution-grown colloidal QDs with an organic capping layer, this chapter describes both the inorganic crystal with its electronic structure (2.1), the organic ligand shell and the interplay between these two at the surface-ligand interface (2.2).

2.1 The inorganic nanocrystal

2.1.1 Band theory

The first consequence of reducing the crystal volume of a semiconductor to the nanoscale is that the electronic structure as described by the density of states (DOS) changes significantly. The DOS represents the amount of quantum states in a given energy range that an electron in the crystal can occupy. It is obtained by combining the atomic orbitals of all the atoms in the crystal into molecular orbitals, essentially considering the crystal as a single, very large molecule.

In a bulk semiconductor crystal, two virtually continuous bands of molecular orbital energy levels are formed. This is displayed on the left side of figure 2.1. The band of lower energy, also called valence band (VB), consists of all the states that are occupied when no electrons are excited. The higher energy conduction band (CB) consists of all the unoccupied states. In between the filled VB and the empty CB is an energy range without any states called the band gap. The magnitude of this band gap is denoted E_g and equals the energy difference between the top state of the VB, the highest occupied molecular orbital (HOMO), and the bottom state of the CB, the lowest unoccupied molecular orbital (LUMO).

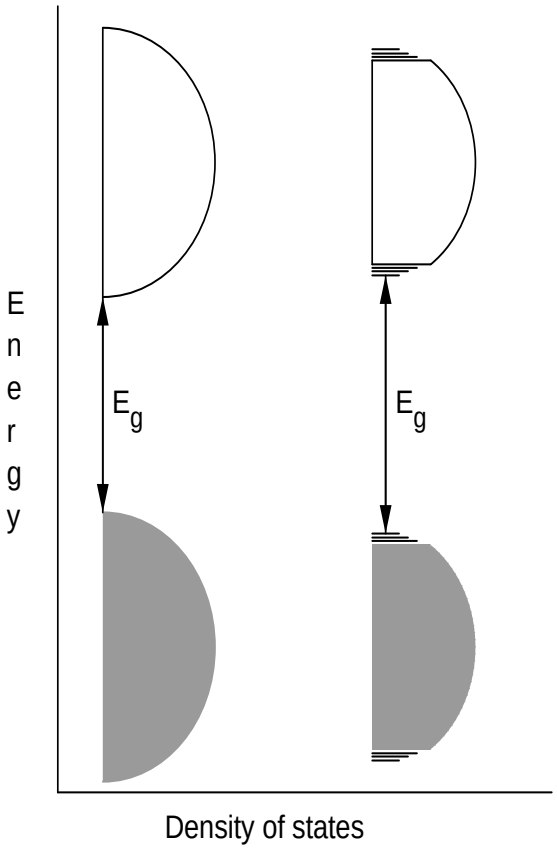

Figure 2.1: *A schematic view of the density of states for a bulk crystal on the left and for a QD on the right. Redrawn from [13].*

A nanocrystal (NC) on the other hand consists of a significantly smaller number of atoms than its bulk analogue and therefore has a DOS intermediate between that of a bulk crystal and the discrete case of a single molecule. The DOS of a QD is displayed on the right side of figure 2.1. As the amount of molecular orbitals suffices only at the center of the bands to maintain a quasicontinuum, the states near the band edges become clearly discrete. The HOMO also shifts down in energy while the LUMO shifts up, which corresponds to an increase in E_g. Strictly speaking, the gap indicated by E_g is no longer a band gap but a gap between the discrete HOMO and LUMO. As the size of a semiconductor NC is decreased, the shifts become more pronounced and the width of the gap increases.

2.1.2 Quantum confinement

The changes in the magnitude of the band gap E_g are reflected in the photoluminescence (PL) of QDs. As illustrated by figure 2.2, an electron can be excited from the VB to the CB under absorption of a photon with energy equal to or greater than E_g. Conversely, a photon of energy E_g may be emitted when an electron from the CB recombines wih a hole in the VB. The energy E of a photon is related to its frequency ν and wavelength λ, and thus the colour of the light, by:

$$E = h\nu = \frac{hc}{\lambda} \qquad (2.1)$$

where h is the Planck constant and c the speed of light. As the QD size decreases, the band gap increases and shorter wavelengths of light are absorbed and emitted.

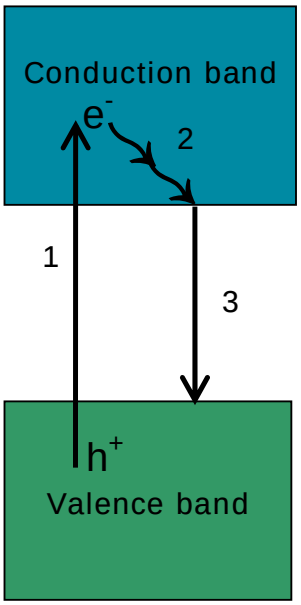

Figure 2.2: *schematic illustration of electron transitions upon (1) photon absorption, (2) relaxation through lattice vibrations, and (3) photon emission.*

Figure 2.2 also shows that an excited electron will leave an empty state in the VB that is called a hole. Holes are mobile and can be described as positively charged quasiparticles, denoted h^+. Because an electron has a negative charge, there will be a Coulomb attraction between an excited electron and the hole that it left. The thus created electron-hole pair forms an exciton, a quasiparticle that is described by a single wavefunction.

If the size of a NC is comparable to the spatial extension of the exciton wavefunction, the exciton is said to be confined in the crystal. This implies that due to the limited size of the NC, the exciton occupies a smaller volume than it would in a bulk crystal. As a result its kinetic energy increases, which translates to an increase in the band gap as mentioned in the previous section. The spatial confinement of electron and hole wavefunctions can thus be seen as the origin of these effects on the electronic structure of an inorganic NC.

By describing quantum confinement of excitons with a 3D particle-in-a-box model, an expression can be derived for the energy of the lowest excited state [5][14]:

$$E_g(r) = E_g(\infty) + \frac{h^2}{8r^2}\left[\frac{1}{m_e^*} + \frac{1}{m_h^*}\right] - \frac{1.786e^2}{\varepsilon r} + E^{pol} - 0.248E^*_{Ry} \qquad (2.2)$$

where $E_g(\infty)$ is the bulk band gap, m_e^* and m_h^* are the effective masses of the electron and hole, e is the elementary charge and ε the dielectric constant of a spherical QD with radius r. The second term in equation 2.2 represents the confinement energy while the third term accounts for Coulomb interaction between the electron and hole. E^{pol} is a combined contribution from the electron and hole self-polarisation energies and E^*_{Ry} represents the exciton Rydberg energy. Although this equation agrees with the band theory of QDs by implying that E_g increases as r decreases, for CdTe QDs better quantitative agreement is achieved with a semi-empirical formula based on tight binding calculations and experimentally determined parameters [15]:

$$E_g(d) = 1.596 + \frac{1}{0.137d^2 + 0.206} \qquad (2.3)$$

with d the QD diameter in nm and E_g the band gap in eV. This equation provides a means of experimentally determining the size of CdTe QDs, as E can be found from absorption spectra.

2.1.3 Non-radiative relaxation due to crystal imperfections

In the discussion so far, it has been assumed that the inorganic NC is of perfect quality. Here, crystal quality is defined as the extent to which enthalpy is minimized by the ideal arrangement of atoms and bonds in each unit cell. A crystal of perfect quality thus has no defects, both in the interior and on the surface. For such crystals, there are no quantum states in the band gap so that figure 2.2 gives a complete picture of PL behavior.

However, truly perfect crystals do not exist outside of theory. Firstly, any bare crystal of finite size has unsatisfied bonds at the crystal facet surfaces. For this reason a surface can be described as a plane defect. Whereas atoms in the interior or bulk of the inorganic crystal have sufficient neighbours to bind all their valence electrons (unless they happen to flank a vacancy), atoms at the surface have a lower coordination number, leaving them with unsatisfied bonds protruding from the surface. As shown in figure 2.3, this introduces defect states in between the VB and the CB which are referred to as surface states. A more detailed discussion of surface states of colloidal NCs is given in paragraph 2.2, including ways in which they can be passivated, i.e. shifted out of the bandgap.

Secondly, crystallographic defects such as point defects and line defects are expected. This can be understood by considering free energy minimization:

$$G = H - TS \tag{2.4}$$

Although creation of a defect in the lattice increases enthalpy H, it may also increase the entropy S and may thus lead to an overall decrease of free energy G. The gain in entropy will be very high for the introduction of the first defect in an otherwise perfect lattice. For this reason some defects are expected in any crystal at $T > 0$ K, even in thermodynamic equilibrium. These defects can be in the interior as well as on the surface of the crystal, and give rise to trap states in between the VB and the CB as illustrated in figure 2.3. Although both unpassivated surface states and trap states originate from defects, due to the different nature of these defects trap states are often found deeper in the band gap. In a high-quality crystal the number of entropy-driven defects is usually small, limiting the amount of trap states, but NCs which are not in equilibrium are likely to have more crystallographic defects.

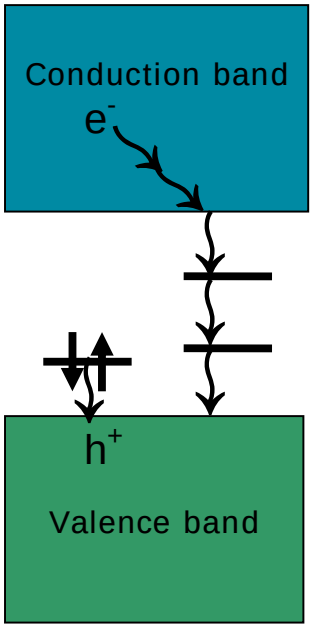

Figure 2.3: *A schematic illustration of PL quenching by trap states in an excited QD. The wavy arrows indicate relaxation by emission of a phonon. In other words, the released energy is dissipated to the lattice, facilitating non-radiative recombination of the electron and hole.*

The presence of defect states enables alternative, non-radiative pathways for an excited electron to recombine with the hole. As illustrated by figure 2.3, the energy difference between surface or trap states and the band edges may be so small that relaxation can occur thermally, in other words, by release of energy as lattice vibrations. Under emission of a phonon the excited electron may thus relax from the CB to a state in the band gap and eventually to the VB. Similarly, the hole may occupy a defect state, in which case an electron effectually moves to the VB from the state. In either case, when an excited charge carrier relaxes into such a state, its wavefunction is localized which reduces the probability of recombination with a carrier of opposite charge. Instead, coupling with phonons will relax the exciton under emission of heat rather than a photon.

In some instances, an exciton of which the hole or electron is trapped can still recombine radiatively. Because this involves a transition between a defect state and a band edge instead of between the two band edges, the emitted photon has less energy than the band gap E_g. For this reason, such defect-related emission is visible in the PL spectrum as a broad peak at longer wavelengths than the excitonic emission. The intensity of this defect emission peak does not fully reveal the quality of the excited NCs, because it does not contain any information on the extent of non-radiative recombination.

2.1.4 Quantum yield as a measure of crystal quality

A more useful way to evaluate crystal quality is by measuring the photoluminescence quantum yield (QY). In the complete absence of non-radiative decay, each photon absorbed by the NC will eventually result in an emitted photon. This ratio between photon input and output is then referred to as the QY:

$$\mathrm{QY} = \frac{\text{number of photons emitted}}{\text{number of photons absorbed}} \tag{2.5}$$

For an ideal NC the QY will be 1. In practice, however, there are multiple factors that cause deviation from this ideal situation. Essentially, it is the quality of the crystal and most importantly its surface [16] that determines the extent of PL quenching. This quality is influenced by the journey of the QD over the free energy landscape, which in turn is influenced by an interplay of factors such as temperature, concentration, type of solvent, exposure to light, and importantly the type, amount and distribution of coordinating ligands, as will be discussed in the next paragraph. Note that there is no driving force for the crystal to maximize its PL QY per se: any outcome merely happens to coincide with the actual driving force of free energy minimization.

Although the above description is valid for single QDs, it is important to note that measurements of QD ensembles only produce results that are averaged over the entire population. Some percentage of the dots is expected to be completely dark or ‘dead’, never emitting any visible photons but instead converting all absorbed energy into heat by non-radiative decay. The dots that do emit radiatively, generally do so intermittently. On a timescale between milliseconds and seconds, they blink between on and off states. For example, a measured QY of 16% could originate from half of all NCs being completely dark, with the other half being in the ‘on’ state for 80% of the time, while in this state emitting light with an average QY of 40% due to the factors mentioned above. Such blinking behavior also averages out in measurements of large scale ensembles as performed in this work. It can be observed in experiments with single QDs using for example confocal microscopy. [17]

2.2 The ligand-capped surface

2.2.1 Influence of the surface on NC properties

Reduction of the inorganic crystal volume to the nanoscale has a second set of consequences, stemming from the increase in surface-to-volume ratio rather than from spatial confinement of wavefunctions as described in the previous paragraph. Assuming spherical[2] crystals of radius r, the surface-to-volume ratio S (unit m^{-1}) of a crystal is given by:

$$S = \frac{4\pi r^2}{(4/3)\pi r^3} = \frac{3}{r} \tag{2.6}$$

Upon reduction of the radius r, it is seen that the ratio S will increase. Especially as r reaches very small values this increase will become significant, since equation 2.6 goes to infinity in the limit that r approaches zero. This means that the surface-to-volume ratio is very sensitive to changes in r in the nanoregime but much less so for macroscopic crystals. Thus, in NCs a significant fraction of atoms is at the surface, whereas in bulk crystals this fraction approaches zero. This means that the surface becomes of great importance to the identity of a NC, affecting its overall properties. For example, since atoms on the surface have a higher free energy, NCs will have a lower melting point as the fraction of surface atoms increases. [1] Equation 2.6 also implies that slight differences in the radii of NCs may result in large differences in observable properties due to variations in the significance of surface effects. From this it becomes clear that any description of a NC is incomplete without considering the influence of the surface.

2.2.2 Colloidal stabilization through ligands

As mentioned in section 2.1.3, any bare crystal of finite size has unsatisfied bonds at the crystal facet surfaces. The fraction of unsatisfied bonds increases with the surface-to-volume ratio, so that colloidal NCs experience strong surface tension. A NC will evolve to a state where this surface tension is minimized, insofar as this is kinetically possible.

In principle, collective aggregation of NCs into a macroscopic crystal is the best method to minimize surface tension. As this would eliminate the nanoscopic nature of the QDs, methods have been developed to prevent such aggregation by imposing energy barriers. A simple solution would be to immobilize the QDs in a substrate such as glass, but this is not practical for many experiments. A good way to stabilize colloidal QDs in a liquid medium such as toluene is capping of the surface with coordinating ligands. Some ligands have long carbohydrate chains that stick out from the QD surface and keep other QDs at a distance by steric hindrance, thus preventing aggregation. Other, charged surfactants create an energy barrier by Coulomb repulsion. The CdTe QDs used for the experiments in this thesis were synthesized in a mixture of trioctylphosphine (TOP) and dodecylamine (DDA), as detailed in the experimental section. Figure 2.4 shows the molecular structure of these ligands. TOP and DDA coordinate preferentially to Te and Cd atoms on the surface, respectively, and prevent aggregation of NCs by steric hindrance.

[2] It should be noted that an actual QD can never be perfectly spherical – this is in fact physically impossible due to the crystal structure and the finite number of atoms it is composed of. A more accurate description could be obtained by counting the fraction of atoms at the crystal surface, also referred to as the dispersion. However, this is a more complicated procedure and the spherical approximation is an adequate way to demonstrate the key point that surface becomes more important as crystal size is reduced.

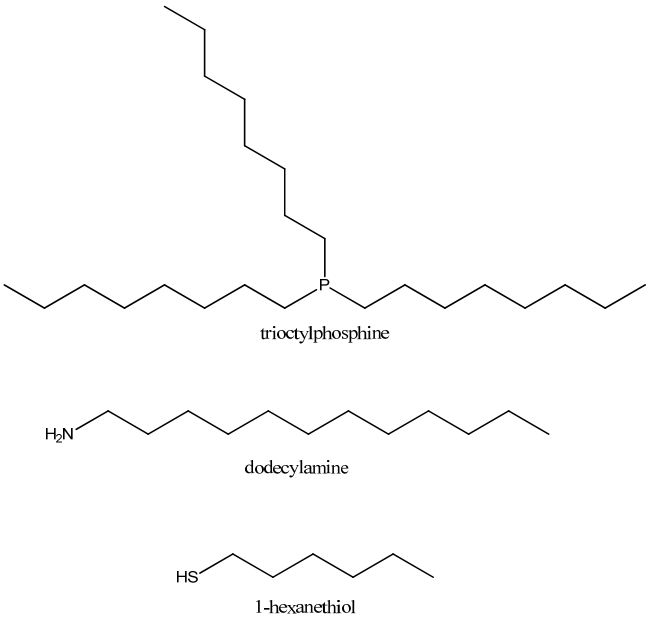

Figure 2.4: *Structures of three commonly used ligands for stabilization of CdTe QDs.*

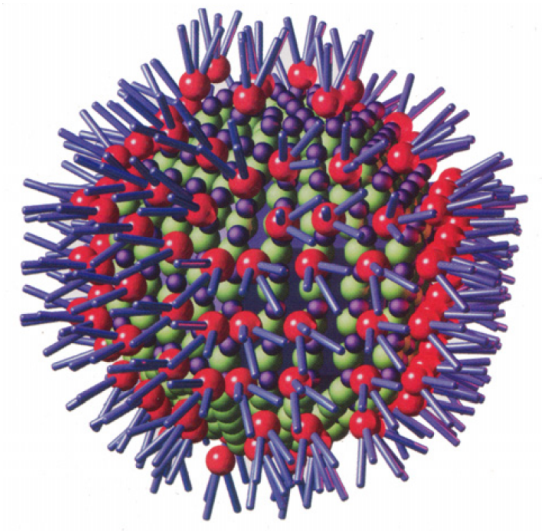

Figure 2.5: *Model of a CdTe QD capped with TOP molecules. Image courtesy of P. Schapotschnikow (TU Delft).*

2.2.3 Surface passivation

With organic ligands preventing the aggregation of colloidal NCs, other processes manifest to relieve surface tension instead. The very binding of the surfactant head groups to inorganic atoms can in itself passivate surface states, i.e. cause them to shift outside the band gap[3]. Efficient passivation through ligand binding requires optimal coverage of the surface, as each inorganic atom with unsatisfied bonds must bind to an organic head group.

Although full coverage of the surface minimizes the free energy for the inorganic crystal G_{NC}, it may have a contrary effect on the free energy for the surfactant shell G_{SS}. For example, coverage of each crystal atom with TOP would cause the total free energy G_{tot} to rise due to strain between the alkyl chains of the bulky ligands. As seen in figure 2.5, many surface atoms of a TOP-capped NC are therefore left uncovered. The linear nature of molecules such as DDA makes these surfactants better suited for achieving high surface coverage, although coupling between G_{NC} and G_{SS} may still result in ligands imposing unfavourable conditions on the NC if this sufficiently minimizes G_{SS}. A more detailed discussion on the implications of this coupling on the identity of colloidal QDs is given in the next section.

[3] Some organic molecules can also passivate deeper trap states that arise from irregularities on the NC surface. For CdTe QDs, an example of such a ligand is 1-hexanethiol (HT), shown in figure 2.4. When DDA ligands on colloidal CdTe NCs are exchanged for a well-chosen amount of HT, the PL QY increases. The opposite is also possible: HT is known to quench PL of colloidal CdSe QDs by introducing hole traps. [10] These effects have little relevance to the research reported in this thesis and are thus out of scope of the present discussion.

2.2.4 Surface relaxation and reconstruction

Literature on macroscopic crystals describes the relatively simple case of an uncapped or bare surface relieving its surface tension by processes known as relaxation and reconstruction. [18] In a relaxed surface, the outer inorganic atoms are drawn slightly inwards to increase bonding with the underlying layer of atoms. In the case of reconstruction, bond lengths as well as crystal geometry are modified to achieve more efficient bonding. This process is distinguished from relaxation by changes in the periodicity of the surface due to the displacement of atoms. An example of reconstruction is the formation of pairs of atoms on the surface that share their unsatisfied bonds. More extensive forms of reconstruction may also occur, especially in NCs since these consist largely of surface. For colloidal CdSe QDs with a diameter below 4 nm, global reconstruction has been observed in NMR experiments. [19]

Many syntheses produce colloidal QDs that are metastable rather than in thermodynamic equilibrium, because the growth rate of the NCs is still fast when the temperature of the reaction mixture is lowered to end growth. This freezes the crystals in a local minimum, rather than the global minimum of the free energy curve that would be reached with slower growth rates. Chemical procedures such as purification and ligand exchange may also put the system in a metastable state. In such cases, there is potential for further improvement through surface relaxation and reconstruction. Indeed, increases [8, 20, 21] and decreases [7] in the PL QY are often observed in the first days or weeks after synthesis, even for samples stored in a glovebox. However, the full path to thermodynamic equilibrium may well be blocked by the presence of energy barriers that are relatively large compared to the thermal energy at room temperature kT. The organic capping layer can be an origin for such barriers, as will be discussed in the next section.

2.2.5 Influence of the capping layer on NC identity

Although relaxation and reconstruction are well-understood for uncapped surfaces, the presence of organic ligands on colloidal NCs introduces additional complexity. Different ligands may steer these processes in different directions, since they contribute to shaping the free energy landscape through their bonds with surface atoms. In other words, for a colloidal QD there is a coupling between the free energy function of the inorganic and the organic components. Changes that would not normally occur in a component if it were separate, will be facilitated if they sufficiently lower the free energy of the whole. The inverse also holds: changes that would normally occur in a seperate component could be blocked due to the influence of the other component. For example, the bare surface of a macroscopic crystal is known to relax spontaneously, but for ligand-capped NCs there may be an energy barrier.

This essentially involves a competition between the inorganic crystal and the ligand shell to dominate the free energy landscape[4]: whichever has the most significant contribution to the total free energy function, largely determines the location of its minimum. Indeed, TEM observations of PbSe QDs show that the morphology of an inorganic NC can be highly dependent on its capping layer. Whereas capped NCs were found to have spherical multifaceted shapes, these same crystals became cubic with predominantly {100} facets after evaporation of the capping layer in vacuum. [22] Although calculations showed that the {100} surface is indeed the most stable for uncapped PbSe crystals, the presence of ligands had clearly changed the equilibrium shape of these dots. It is thus expected that changes in the capping layer of a colloidal QD can trigger reconstruction of the inorganic NC.

[4] More specifically, the slope of the free energy landscape.

In addition to modifying the equilibrium state, ligand-surface coupling may also transform the path over the free energy landscape towards the minimum by introducing or removing energy barriers. Strong interactions between the alkyl chains of surfactants may result in rigid layers of surfactants, so that displacement of one of the underlying inorganic atoms can only occur at the high cost of either breaking the ligand-surface bond or breaking several ligand-ligand interactions. When energy costs of intermediate steps in surface reconstruction exceed kT, this can kinetically freeze a NC in a metastable configuration until sufficient energy is added to overcome the barrier. Thus, changes in the capping layer of a colloidal QD could simultaneously redefine the global minimum and kinetically block reconstruction towards that minimum, so that observable changes may only manifest at a time when activation energy is supplied to the system.

Reconstruction kinetics are also influenced by the affinity of surfactant head groups for the inorganic surface atoms. Capping ligands form a dynamic layer around the QD: they continually attach and detach from the surface at a certain rate, that tends to decrease with increasing binding strength. Thus, a very strongly binding ligand may provide good passivation but force reconstruction to occur via a pathway in which inorganic atoms are displaced with their ligands still attached. This is not likely the case for amine ligands on colloidal CdTe or CdSe QDs dispersed in a solvent, as these interact with the surface in a very dynamic way. [23] For octylamine on CdSe, an exchange rate of 50 s^{-1} was found in NMR studies. [24, 25] The authors suggest that this implies the entire ligand shell is refreshed[5] at least 3500 times in a time span of 70 seconds. It is also worth noting that exchange rates increase at edges or defect sites on the NC surface, so that these sites are less likely to be kinetically locked in a metastable state. [26, 27]

The role of the capping layer in surface reconstruction is coupled to physical and chemical parameters such as temperature and concentration. Directed manipulation of these parameters allows control over the crystals even without replacing the ligands themselves. This is aptly demonstrated by experiments in which the exciton lifetimes and QYs of amine-capped CdSe QDs increased when the dots were heated above a certain temperature, an effected that was dubbed luminescence temperature anti-quenching (LTAQ). [28, 11, 29] The threshold temperature was found to increase with the alkyl chain length of the primary amine ligands used, suggesting that the measured changes in PL can be traced to a transition of the ligand layer from a solid-like ordered phase to a more fluid phase in which rotational motion is possible. In the solid-like phase, rigid ligands allow too little motion for surface atoms to reconstruct, imposing an unfavourable geometry which leads to surface states in the band gap. Upon heating above the transition temperature, the ligand alkyl chains gain precessional mobility, triggering reconstruction of the NC which shifts surface states out of the band gap. Thus, the QY increases purely by manipulation of the surfactant layer through temperature changes. The experiments reported hereafter demonstrate a different way of manipulating the surface-ligand interface, and a model is presented to explain the underlying mechanism.

[5] This includes re-attachment of the same ligands that had detached a moment before.

3 Experimental methods

3.1 Sample preparation

3.1.1 Materials

Dimethylcadmium ($CdMe_2$) was purchased from ARC Technologies. Tellurium (Te; 99.999%, < 250 μm) powder was purchased from Heraeus. Trioctylphosphine (TOP; ≥ 90%) was obtained from Fluka. Anhydrous toluene (99.8%), dodecane (99%), dodecylamine (DDA; 98%), octadecylamine (ODA; 97%), *n*-Tetradecylphosphonic acid (TDPA; 97%) and 1-hexanethiol (HT; 95%) were bought from Aldrich. Rhodamine B (QE = 90%) was supplied by Exciton. All chemicals were used as received with the exception of DDA and ODA, which were dried under vacuum for several hours at 100 °C.

3.1.2 Synthesis of CdTe QDs

Three batches of colloidal DDA-capped CdTe QDs were used for the experiments, labeled WA2, Ar1 and Ar2. All were prepared from Te powder and $CdMe_2$ by a high-temperature wet-chemical synthesis in TOP. The procedure is based on work by Murray et al. [30] with modifications by Talapin et al. [31] and Wuister et al. [32]. The QDs denoted as WA2 were synthesized in cooperation with Ward van der Stam, 1 year prior to the reported experiments. Batches Ar1 and Ar2 were synthesized at least 6 and 3 months prior to the reported experiments, respectively. All syntheses were carried out in a nitrogen-filled glovebox.

As an example the synthesis of WA2 is described. Under constant stirring, 7 mL of TOP was heated to 45 °C after adding 10 g of DDA. After adding another 7 mL of TOP containing 0.22 g or 1.54 mmol of $CdMe_2$, a small volume of toluene was used to transfer 0.163 g or 1.25 mmol of Te powder to the flask. The mixture was stirred at 50 °C for 20 minutes, during which it appeared slightly green due to dissolving Te. Upon increase of the temperature to 145 °C, a white vapour emanated which is ascribed to decomposition of $CdMe_2$. The mixture gradually changed its colour from dark green to reddish. After 140 minutes, a sample was collected and the remaining mixture was heated to 165 °C for another 220 minutes. Weak luminescence was observed upon excitation of the QDs with blue light. After 24 hours the luminescence was more intense.

3.1.3 Washing and recapping of CdTe QDs

The following general protocol was followed for washing. Crude reaction mixture was centrifuged to remove Te powder. After addition of toluene (1:1 v/v), methanol was added dropwise until the mixture became turbid. The suspension was centrifuged for 10 minutes at 2300 rpm, and after removal of supernatant dried in a vacuum chamber. The remaining dry cake was redispersed in a small volume of toluene (for PL measurements) or dodecane (for FTIR).

Recapping of Ar2 dots in 0.6 M DDA and ODA was achieved by mixing 600 μL of washed Ar2 with 160 and 230 μL of pure ligand, respectively. The mixtures were incubated at 40 ºC under stirring for 12 hours.
Recapping of Ar2 dots in 2.0 M DDA and ODA was achieved by mixing 250 μL of the aforementioned 0.6 M concentrate with 152 μL and 292 μL of pure ligand, respectively. The mixtures were incubated at 55 ºC under stirring for 12 hours.
Recapping of Ar2 dots in 4 M DDA and ODA was achieved by mixing 50 μL of washed Ar2 with 1 mL of pure ligand. The mixtures were incubated at 55 ºC under stirring for 60 hours.
Recapping of Ar2 dots in 2.0 M DDA laced with 100 TDPA/QD was achieved by mixing 400 μL of washed Ar2 with 420 μL of pure DDA and 80 μL of a 0.07 M solution of TDPA in toluene. The mixture was incubated at 55 ºC under stirring for 12 hours.

3.2 Spectroscopic methods

Several spectroscopic methods were used to probe colloidal DDA-capped CdTe QDs at various points in time after these were dispersed in toluene. Unless stated otherwise, these dispersions were prepared by adding 100 parts of toluene to 1 part of crude reaction mixture or washed and recapped product. To keep track of the time, a stopwatch or computer clock with an accuracy on the order of a second was used.

3.2.1 UV-visible absorption spectra

Absorption spectra were recorded with a Perkin-Elmer 16 UV/vis spectrometer against a reference from the same toluene source. Unless otherwise stated, spectra were baseline corrected but not normalized.

3.2.2 Photoluminescence spectra

Emission spectra were recorded with a liquid nitrogen cooled CCD-camera of 1024 by 256 pixels, type Princeton Instruments LN/CCD-1024-EB/1, controlled by a PI ST133 system and linked to a 0.3 m Acton Research Spectra Pro 300i monochromator with a grating of 150 lines/mm blazed at 500 nm. The QDs were excited by a light emitting diode (LED) with a maximum intensity at 400 nm, of which the spectrum is shown in figure 3.1.

Fibers were used to couple the light from the outside source to a custom-built sample holder inside a glovebox, and likewise to bring the emitted light from the sample inside the box to the camera outside. This setup, schematically depicted in figure 3.2, serves to exclude the possibility that the temporal evolution of the PL spectra is affected by oxidation of QDs. The connection points for fibers allow reproducible measurements to be carried out over several days. In order to minimize the influence of reabsorption of emitted photons on the obtained PL spectra, the excitation beam was directed to the side of the cuvet close to the light collecting fiber, as shown in figure 3.2.

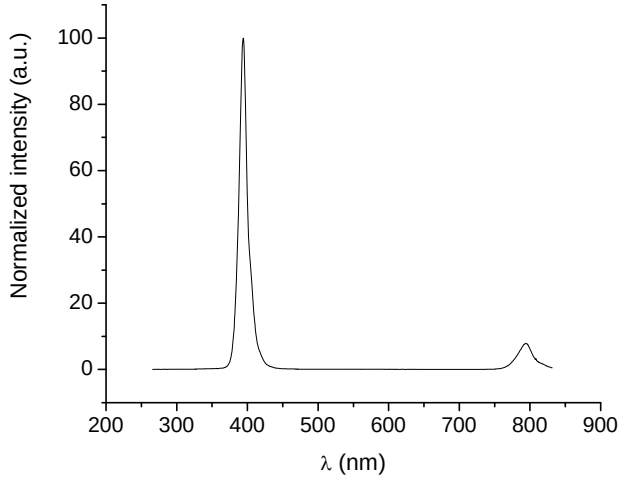

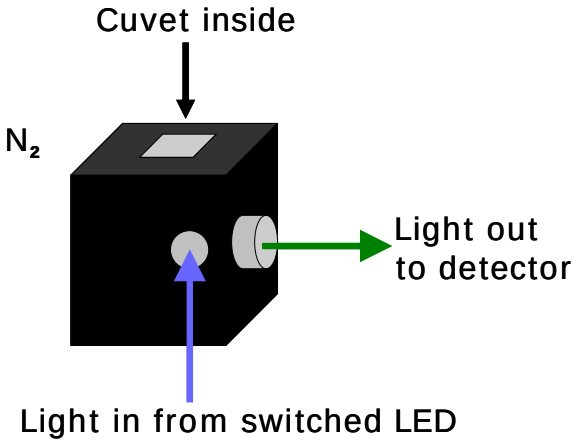

Figure 3.1 (left): *Spectrum of the 400 nm fiber-coupled LED used as excitation source for PL measurements. This is the spectrum measured inside the glovebox, in the same configuration as used for all experiments.*

Figure 3.2 (right): *Home-built sample holder for measurements inside a nitrogen-filled glovebox. Light input and output is directed by fibers. The cap that closes the holder's top is not shown.*

To observe the PL of the colloidal DDA-capped CdTe QDs as a function of time, series of emission spectra were recorded by periodically switching the excitation source and CCD-camera on at a specified interval of 5 or 10 minutes. This was done automatically by the ST133 controller configured through Roper WinSpec/32 software version 2.4.7.5. In between measurements, the sample was kept in darkness: the LED was switched off and environmental light was blocked by a cap over the sample holder.

The automated measurements produced large series of consecutive emission spectra, which were analysed in one of two ways. The first method, used for all series except the ones with washed and recapped dots, consisted of numerical integration between two points on the wavelength axis. These integration bounds were kept constant among all frames of a given series. The data point with the maximum amount of counts in this integration interval was taken as the peak maximum. FFT smoothing of spectra was employed to obtain a more stable evolution of the peak maximum. Analysis comparisons were performed to ensure that the smoothing and boundary choice did not arbitrarily affect the results of the analysis.

Because the emission spectra of washed and recapped Ar2 dots contain two peaks – excitonic and defect emission – with significant overlap, integrating between fixed boundaries is not accurate with these samples. For integration of these spectra, a Mathematica script was used to fit a sum of two Gaussians through each spectrum, using the formula:

$$\Phi = B_0 + \frac{A_1}{s_1\sqrt{2\pi}}\,\exp\left[-\frac{(1-L_1)^2}{2{s_1}^2}\right] + \frac{A_2}{s_2\sqrt{2\pi}}\,\exp\left[-\frac{(1-L_2)^2}{2{s_2}^2}\right] \tag{3.1}$$

where Φ denotes the detected photon flux (counts/s), B_0 the baseline, A_1 and A_2 the areas of the fitted Gaussians for the excitonic and defect emission, respectively, and L_1 and L_2 the wavelength maxima of the fitted Gaussians. The parameters s_1 and s_2 are related to the full width at half maximum (FWHM) of the fitted Gaussian peaks by:

$$\mathrm{FWHM} = \sqrt{8\ln 2}\times s \tag{3.2}$$

3.2.3 Photoluminescence quantum yields

Equation 2.5 defines the photoluminescence quantum yield (QY) as the ratio between the number of absorbed and emitted photons. Because these quantities are hard to measure directly, indirect methods were used. The relative QY of a sample with respect to a reference dye was determined by measuring the absorption and emission spectra of both the sample and the standard. The following equation then gives the sample QY q_X within an error of ±10% : [33]

$$q_X = \frac{1-T_{ST}}{1-T_X}\times\frac{\Delta\Phi_X}{\Delta\Phi_{ST}}\times q_{ST} \tag{3.3}$$

Here, $\Delta\Phi_X$ and $\Delta\Phi_{ST}$ denote the measured integrated emitted photon fluxes of the sample and dye, respectively. The areas of the emission spectra can be used for these quantities, provided that the spectra of sample and dye were acquired under the same experimental conditions. The QY of the dye standard q_{ST} was 0.9 for the solution of Rhodamine B in absolute ethanol that was used in all PL experiments that included a dye. The terms T_{ST} and T_X denote the transmittances of the standard and sample, respectively, at the excitation wavelength of 400 nm. These were calculated from the absorbance A at 400 nm measured in absorption spectra:

$$T = 10^{-A} \tag{3.4}$$

3.2.4 Photoluminescence decay curves

Decay curves were obtained by time correlated single photon counting (TCSPC) using a PicoQuant LDH-C 400 pulsed diode laser with PDL 800-B driver. The laser beam had a wavelength of 406 nm, pulsewidth of 55 ps and repetition rate of 2.5 MHz. Through a 0.1 m Bausch & Lomb monochromator of 1350 grooves/mm and 500 nm blaze, the emission from the QDs was passed to a Hamamatsu H5738P-01 photomultiplier tube. Pulse height analysis was performed by a Time Harp 200 multichannel computer card. By using Lambda Physik neutral density filters the photon yield was kept below 4% per pulse as registered by the computer card. Decay curves were first normalized and subsequently baseline corrected.

3.2.5 Dynamic light scattering

In order to detect any formation or breaking down of QD clusters in dispersions of DDA-capped CdTe QDs, DLS measurements were performed with a Malvern ZetaSizer Nano using ZetaSizer software 6.20. The sample dispersion was prepared by adding 100 parts of toluene to 1 part of Ar2 crude reaction mixture in a nitrogen-filled glovebox. It was filtered twice with a hydrophobic 0.2 μm Whatman syringe filter to remove dust particles. Within 30 minutes after the addition of toluene, the sample was brought to the DLS instrument in a quartz cuvet sealed with a plastic cap, PTFE tape and parafilm. The sample temperature was kept at 25 degrees during the measurements by the instrument's built-in thermostat. Backscatter was measured at an angle of 173 degrees, while forward scattering was measured at an angle of 12.8 degrees. Fits were obtained with the ZetaSizer fit model based on multiple narrow modes. After finishing the DLS measurements, an absorption spectrum of the sample was acquired to confirm that the particles had not been oxidized.

3.2.6 Fourier Transform Infrared spectroscopy

In order to obtain information on the concentration and chemical environment of DDA capping ligands, Fourier Transform Infrared (FTIR) spectroscopy was performed with a Perkin Elmer Frontier spectrometer. Two experiments were performed. For both, dodecane was used as a solvent instead of toluene to avoid saturation around regions of interest near 1600 cm^{-1}. Dispersions of washed DDA-capped WA2 product were injected in a transmission cell consisting of two KBr windows with a chamber for approximately 10 μL of liquid in between. The path length of this cell was 100 μm. After injection, the cell was sealed with PTFE plugs and taken from the glovebox to the spectrometer's chamber within 5 minutes. The oxygen and water concentrations in this chamber were kept low by a gentle flow of nitrogen, as confirmed by control FTIR measurements of the gas-filled chamber without the sample inside.

In the first experiment, the validity and sensitivity of the method was determined. Samples were prepared by adding 0.1, 0.2, 0.6 and 0.10 g of DDA to 0.5 mL of washed WA2 in dodecane in a glovebox, followed by vigorous homogenisaton. After 48 hours of equilibration time, all samples showed sedimentation of QDs except for the one to which 0.10 g of DDA had been added. After vigorous shaking to ensure homogeneous samples, IR spectra were acquired.

In the second experiment, the temporal evolution of the FTIR spectrum was measured for DDA-capped WA2 CdTe QDs dispersed in dodecane. 1 mL of washed WA2 in dodecane was colloidally stabilized by adding 0.213 g of solid DDA, followed by vigorous homogenisaton, inside a glovebox. From absorption spectra it was derived that this stock concentrate has a [QD] of 16 μM. The measurement sample was prepared by adding 100 parts of dodecane to this stock concentrate. This dispersion was quickly injected in the transmission cell and brought to the spectrometer. The sample chamber was kept closed and under nitrogen for the entire duration of the experiment.

4 Results and discussion

4.1 PL enhancement of DDA-capped CdTe QDs

4.1.1 Optical properties of DDA-capped CdTe QDs

Table 4.1 lists some of the collection conditions of three crude reaction mixtures containing colloidal TOP/DDA-capped CdTe QDs, as well as properties of these QDs determined from absorption and emission spectra. Transmission electron microscopy (TEM) pictures of 1 part of crude WA2 reaction mixture dispersed in 100 parts of toluene were also obtained. As can be seen in figure 4.1, the QDs are visible in these pictures but not very clearly due to the large amount of organic molecules in the unwashed mixture. By measuring 31 QDs on various TEM micrographs, an estimate of 3.0 nm for the NC diameter was obtained with a standard deviation of 0.7 nm. This is in reasonable agreement with the result from absorption spectra. A slightly larger value is expected from TEM micrographs, as small particles are easily overlooked.
Note that the crude reaction mixtures contain approximately 1.5 M of TOP and 3.0 M of DDA.

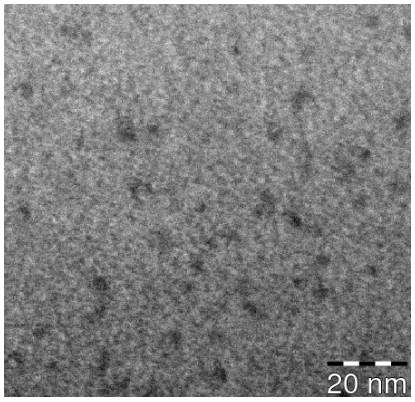

Figure 4.1: *TEM micrograph of WA2 reaction mixture in toluene.*

Table 4.1: *Reaction conditions and NC properties for three different syntheses of colloidal DDA-capped CdTe QDs. The table includes the time after Te addition and temperature at which the mixtures were collected from the synthesis flask. The listed QD concentrations apply to the crude reaction mixtures. Quantum yields were determined 3 minutes after dilution in toluene to a concentration of 0.5 µM (Ar1, WA2) or 1.7 µM (Ar2, after washing and recapping in 2M DDA).*

Sample	Reaction time	T (°C)	QD concentration (mM)	QD diameter (nm)	QY
Ar1-A	2h 15m	165	0.17	2.72	0.14
WA2-D	6h 00m	163	0.22	2.83	0.15
Ar2	2h 40m	150	0.21	2.85	0.19

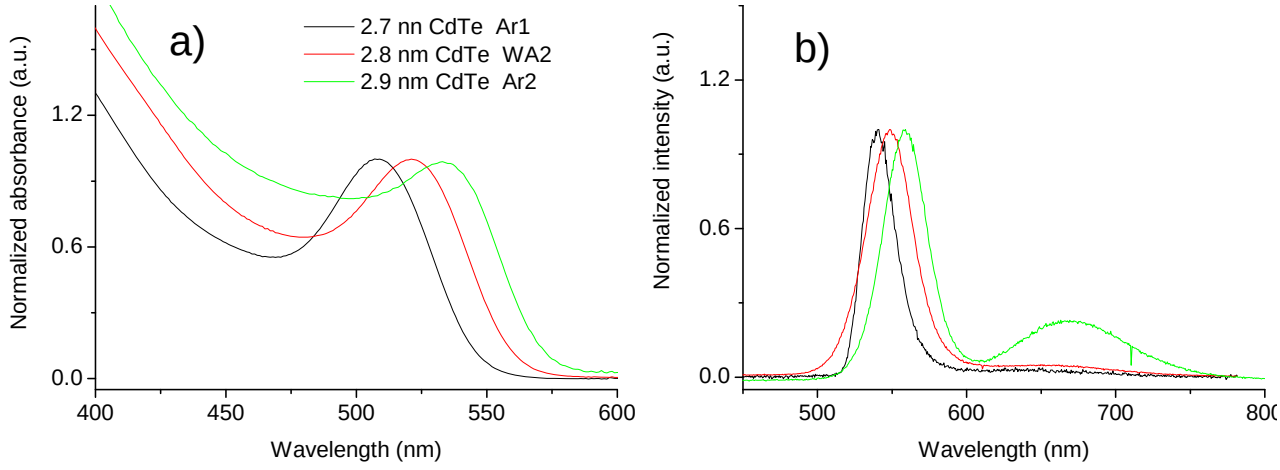

Figure 4.2: *Normalized absorption* ***(a)*** *and emission* ***(b)*** *spectra of colloidal WA2, Ar1 and Ar2 CdTe QDs dispersed in toluene. The Ar2 dispersion contained washed product recapped in 2 M DDA, whereas the Ar1 and WA2 samples were made with crude reaction mixture.*

4.1.2 Temporal evolution of PL in dark dispersions

After dispersion of these colloidal CdTe QDs in toluene, their PL intensity increases with time. This is illustrated in figure 4.3 for three 100x dilutions of crude Ar1 in toluene. However, these particular samples were not thoroughly protected from illumination and oxidation, both of which have been reported to trigger increase of PL intensities under certain conditions. [12]

Thus, to make more interpretable observations, 1 part of washed Ar2 product (with [QD] = 0.17 mM) in 2 M DDA was redispersed in 100 parts of toluene and stored in a closed, dark container in a nitrogen-filled glovebox. A PL spectrum taken directly after dilution was compared to spectra taken at progressive points in time. For each spectrum a new aliquot from the sample vial was used and immediately discarded, so that no sample had been exposed to light prior to the 1 second exposure necessary for obtaining its spectrum. The stored dilution was also carefully sealed to avoid contamination with any molecules in the glovebox atmosphere.

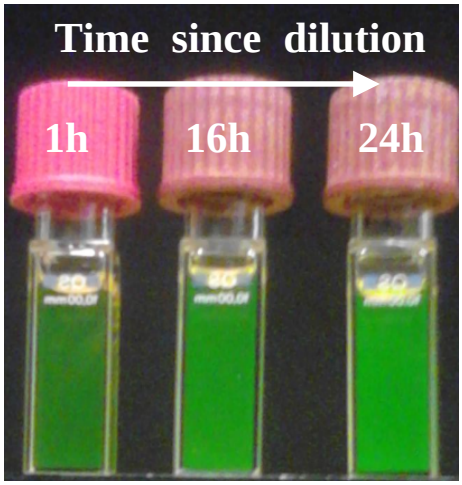

Figure 4.3: *DDA-capped Ar1 CdTe QD dispersions at increasing times since they were diluted from crude stock.*

Figure 4.4a shows that for these controlled experiments, the PL intensity kept increasing over the course of many hours. After 24 hours, the excitonic emission peak area reached 133% relative to the initial frame.

Variations in excitation intensity were controlled for by measuring the spectrum of a Rhodamine B dye solution immediately after each frame, of which the area remained constant within an error of 5%. Most of this error was likely due to small temperature variations in the measurement room: figure 4.4b seems to show an oscillation which returns to unity after 24 hours.

The dye control also presents the opportunity to calculate the relative QY corresponding to each of the frames in figure 4.4a. Thus, the increase in PL intensity is indeed an increase in QY, provided that the absorbance of the QDs at 400 nm has not changed.

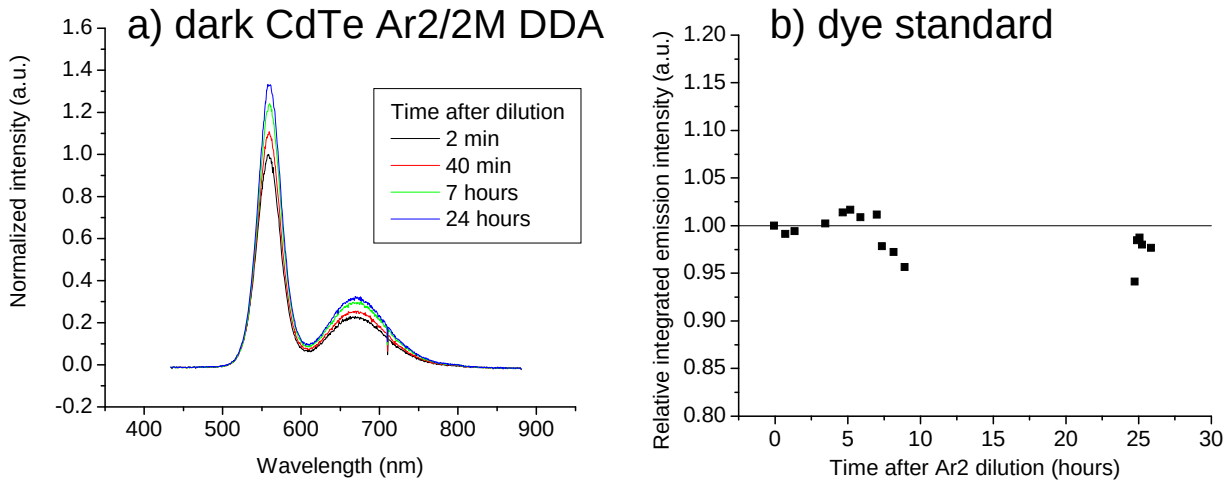

Figure 4.4: ***(a)*** *Emission spectra of washed and recapped CdTe QDs at various points in time since they were dispersed in toluene (1:100). For each spectrum, a new volume of dispersion was used that had been shielded from light since dilution.* ***(b)*** *Fluctuation in the PL intensity of Rhodamine B dye, recorded in between data points of Ar2/2M DDA measurements, remains below 5% - showing the accuracy of the glovebox spectrometer setup.*

4.1.3 Temporal evolution of PL in illuminated dispersions

Much research has been done on PL enhancement of colloidal QDs due to illumination. [12] To evaluate the effect of illumination on the PL enhancement of the colloidal DDA-capped CdTe QDs used in the experiment of section 4.1.2, this experiment was repeated with periodic illumination of the QD dispersion. The sample used to record the first frame of figure 4.4 was kept in a cuvet and exposed to a 1 second flash of the 400 nm LED every 10 minutes. During each exposure, a PL spectrum was recorded. Because these measurements were done on the same day and in the same setup as those for figure 4.4a, the dye control of figure 4.4b also validates these measurements within a 5% margin of error. A selection of the resulting series of spectra in figure 4.6 shows that the excitonic emission peak area reached 138% relative to the initial frame, compared to the 133% that was reached by the dark dispersion.

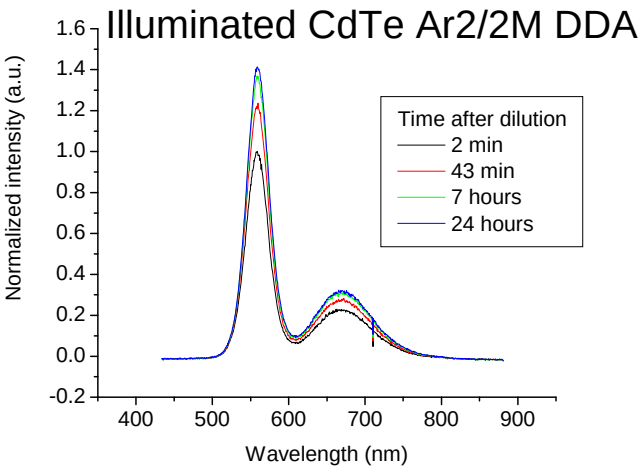

Figure 4.6: *Emission spectra of washed and recapped CdTe QDs at various points in time since they were dispersed in toluene (1:100). The dots were exposed to a flash of 400 nm light for 1 second every 10 minutes.*

The results of figure 4.6 do not reveal whether the higher final PL intensity is due to light-induced amplification of the enhancement effect seen in figure 4.4a, or due to simple addition of two unrelated effects, namely the effect observed in figure 4.4a and additional photobrightening. To investigate whether any interaction exists between light and the effect behind the PL enhancement that occurs even for the dark dispersions, three additional experiments were performed. All three samples were made in the same way: by dispersing 1 part of crude Ar1 reaction mixture in 100 parts of toluene.

In the first experiment, which serves as a reference, the dispersion was exposed to a 1 second flash of the 400 nm LED every 5 minutes for 13 hours. The resulting series of spectra was automatically integrated using a Python script, then normalized by setting the intensity of the first frame to 1. In figure 4.7 the results are shown as blue squares, revealing a trend of rapid enhancement to 126% of the initial frame intensity in the first hour, followed by slower enhancement to a total of 144% after the subsequent 12 hours. This relative increase of the PL QY is somewhat stronger than the 138% found after 24 hours for the purified and recapped Ar2 samples, which may be due to differences in the initial state of the unpurified Ar1 and recapped Ar2 dispersions that cause Ar1 to have a lower initial QY than Ar2, leaving more potential for improvement, and/or due to the presence of TOP in the Ar1 dispersion.

In the second experiment a freshly made dispersion of CdTe QDs was kept in the dark for 24 hours, and subsequently exposed to a 1 second flash of the 400 nm LED every 5 minutes. The results are shown as filled red circles in figure 4.7. In the first 5 minutes a jump to 103% percent of the initial intensity was measured, after which the PL increased slowly in a nearly linear fashion to 106% at 13 hours. To verify that this small increase depends on illumination, the LED flashes were stopped for one hour after 15.5 hours of illumination, at which point the relative intensity was 107%. If the increase had continued linearly during the dark hour, the intensity measured afterwards should be 108%. Instead, it remained 107% as evidenced by the unfilled circle in figure 4.7. Furthermore, some of the dispersion had been kept in the dark during the entire experiment and was measured after 16.5 hours. This dark control, depicted as a crossed circle, shows a relative intensity of only 102% – similar to the enhancement found in the first measurement of the illumination series for this dispersion.

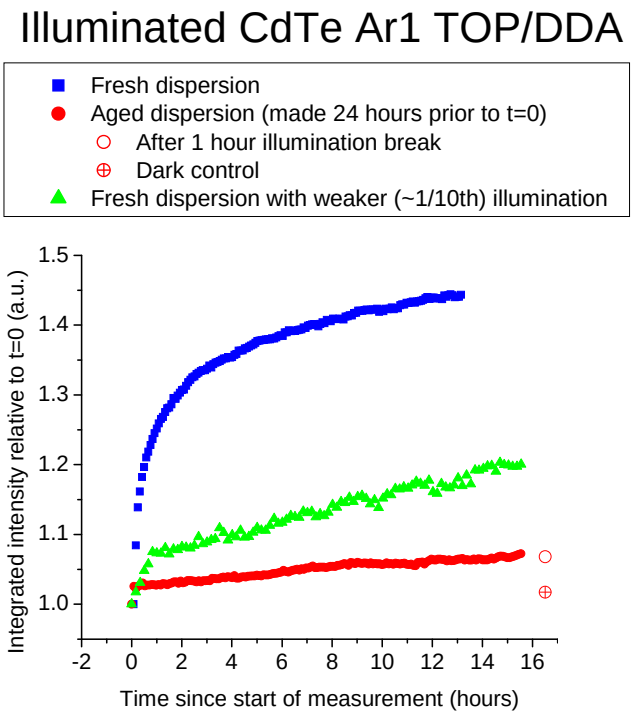

Figure 4.7: *Normalized integrated PL intensities for three CdTe QD dispersions which were made in identical ways from crude Ar1 reaction mixture. A freshly diluted sample (blue squares) brightens rapidly when exposed to a short flash of 400 nm light every 5 minutes. When the light intensity is reduced by a factor of ~10 (green triangles) less rapid brightening is observed. When the dispersion is allowed to age prior to illumination (red circles), only weak nearly linear PL enhancement is observed.*

In the third experiment, a fresh dispersion was made as in the first, but it was exposed to weakened[6] flashes of light at an interval of 10 minutes rather than 5. The green triangles in figure 4.7 show that the PL of the weakly illuminated sample increased in a nearly linear fashion to 107% of its initial value after the first hour, then proceeded on a track of further approximately linear enhancement with a less steep slope. Interestingly, the final slopes of the two freshly diluted samples seem to be identical, suggesting that in the latter stages of enhancement, the intensity of illumination plays a less important role.

[6] By assuming a linear dependence of the emission intensity on the excitation intensity and comparing the absolute intensities of the PL spectra from both experiments after 10 minutes, the intensity of the excitation light was estimated to be 10% of that in the first experiment. This estimate is supported by the relative intensities of excitation light that was scattered towards the detector from the cuvet used in both experiments.

In light of the results from the first and second experiment, a final experiment was performed to determine if identical PL enhancement to the first experiment could be achieved by providing identical amounts of illumination in a shorter period of time. To this end, the first Ar1 experiment was repeated with uninterrupted illumination from the 400 nm LED. Figure 4.8 compares the results of both experiments. Although the constantly illuminated sample rises very fast on the real timescale (not shown), on the cumulative illumination scale the periodically illuminated sample rises faster. In order words, the colloidal CdTe QDs that are given time in between each flash of light show stronger PL enhancement at equal amounts of illumination. This shows that time is an important factor in the enhancement effect under investigation.

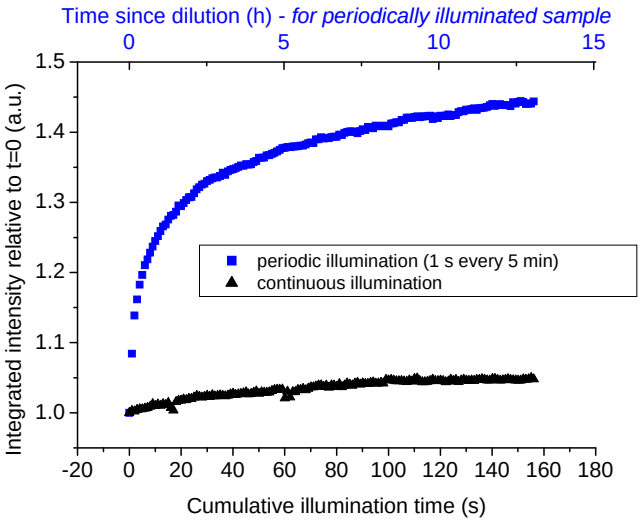

Figure 4.8: *Normalized integrated PL intensities for two CdTe QD dispersions which were made in identical ways from crude Ar1 reaction mixture. The periodically illuminated sample (blue squares) equals the first experiment of figure 4.7. For this sample, 1 second is added to the cumulative illumination time every 5 minutes since dilution. For the continuously illuminated sample (black triangles), the time since dilution equals the cumulative illumination time.*

4.1.4 Temporal evolution of PL decay

Only preliminary results are available from time-resolved measurements of the PL of freshly dispersed CdTe QDs. The PL decay curves in figure 4.9 were obtained with TOP/DDA capped WA2 CdTe QDs dispersed in toluene. A small decrease in the PL lifetime is observed for this particular sample as time after dilution progresses.

Interpretation of these results is hampered by the fact that the samples were irradiated with UV radiation ($\lambda \geq 300$ nm) in an absorption spectrometer shortly after the 1h25m and 2h15m measurements. The largest changes in the PL spectra of figures 4.4a and 4.6 occur in the first hours after dilution. Hence, if a correlation of the decrease in lifetime with PL enhancement should exist, the largest changes in lifetime would be expected in the earliest decay curves. Comparison of the decay curves after 1h and 1h25m (figure 4.9, top right) therefore seems to suggest that there is no such correlation. The changes in subsequent decay curves may have resulted from damage to the QDs by the aforementioned UV irradiation.

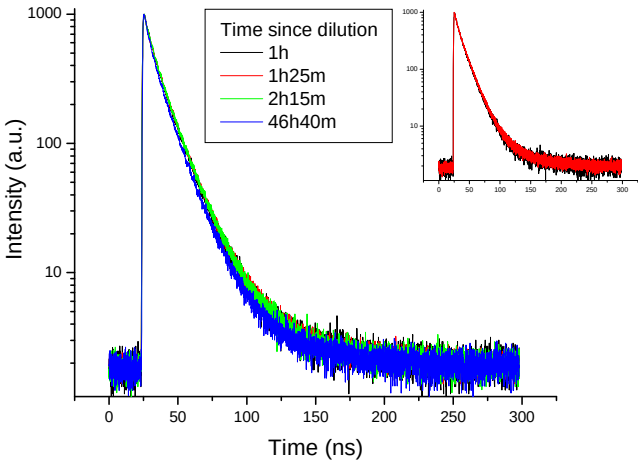

Figure 4.9: *PL decay curves for WA2 CdTe QDs dispersed from the crude reaction mixture in toluene (1:150) show a decrease in the PL lifetime after dilution. Comparison of the first two curves (top right) reveals no significant difference, suggesting that the differences measured afterwards may be artefacts.*

In conclusion, PL decay curves acquired 1h and 1h25m after dilution of TOP/DDA capped WA2 CdTe QDs in toluene provide no evidence for changes in the lifetime. It is advised that these experiments are repeated in a more careful way and starting at an earlier time after dilution.

4.2 Investigation of mechanisms for PL enhancement

Many studies have reported changes in the PL intensity of organically capped colloidal QDs after dispersion in a solvent such as toluene, chloroform or hexane, for which various explanations were offered. Because the PL is highly dependent on the NC surface structure, changes in PL properties are often interpreted to track processes at the NC surface-ligand interface such as surface reconstruction. However, several other mechanisms are known to affect PL properties of QDs in colloidal dispersions. In this paragraph, their relevance to the interpretation of our observations will be discussed, supported by various pieces of additional experimental evidence. A more elaborate investigation on the role of reconstruction of the NC surface-ligand interface is presented in paragraph 4.3.

4.2.1 Role of solvent impurities

All PL measurements reported in the previous paragraph were carried out in a glovebox filled with dry nitrogen. However, both PL enhancement and quenching have been ascribed by several authors to impurities in solvents, such as oxygen or water, adsorbing to and possibly reacting with the surface of colloidal QDs. [8, 34, 35] Even if impurities are only present in trace amounts, dispersion of a small volume of QDs in a large volume of solvent might introduce sufficient impurities to cause noticable changes in the PL. In one remarkable study, PL enhancement was reported for chloroform-dispersed CdSe QDs capped with tri-n-octylphosphine oxide (TOPO) and TOP, that were kept in the dark. [34] No changes in the emission or absorption wavelengths were observed. The particles had a diameter below 3.2 nm, similar to the CdTe QDs used for our experiments. Increased passivation of the surface by adsorbed oxygen molecules was proposed as a mechanism for the enhancement.

Although it is hard to completely exclude the effects of solvent impurities, oxidation of the CdTe QDs is an unlikely explanation for the observed enhancement described in paragraph 4.1. As a test, dispersions of crude WA2 and Ar1 reaction mixture in toluene were exposed to air for 2 seconds within 5 minutes after dilution. After 12 hours, significant quenching of the PL was observed, sharply contrasting the enhancement shown in figures 4.4a and 4.6. Furthermore, the majority of PL changes ascribed to solvent impurities in literature seems to involve chloroform rather than toluene. Moreover, experiments discussed in paragraph 4.3 show a dependency of the PL enhancement effect on variables which is hard to explain under the assumption that impurities in the solvent cause this enhancement.

4.2.2 Relevance of reabsorption assessed from emission spectra

Mei et al. report PL spectra for four different dilutions of hexadecylamine (HDA) capped colloidal ZnSe QDs in butanol and methanol. [36] With increased dilution, enhancement of PL intensity is observed as well as a blueshift of the PL wavelength. This is attributed to a decrease in reabsorption of emitted light, which is a form of energy transfer that leads to PL quenching due to its inefficiency.

Reabsorption is known to cause a redshift in the PL spectrum, as light emitted by smaller QDs, having a wider bandgap, can be absorbed by larger QDs but not vice-versa. A decrease in reabsorption, then, should be accompanied by a reversal of this redshift in the PL spectrum. As figure 4.4a and 4.6 show that there is no such blueshift of the PL for the DDA-capped CdTe QDs investigated in this thesis, the explanation offered by Mei et al. does not seem to apply to our results. Further analysis of shifts in the exciton emission energy is given in paragraph 4.3.

Moreover, reabsorption effects are expected to cause continued evolution in the PL properties of a dispersion of colloidal QDs only as long as this dispersion is inhomogeneous. All samples were homogenized immediately after dilution.

4.2.3 Potential presence of QD aggregates assessed by DLS

Komoto et al. have reported oscillations in PL intensity for TOPO-capped CdSe/ZnS core/shell QDs, concurrent with gradual aggregation of the colloids when dispersed in toluene. [37] A redshift in the PL wavelength was observed, as well as an increase in the average hydrodynamic radius measured by dynamic light scattering (DLS). The oscillations did take place in dark samples but were promoted by illumination. The authors suggest that photodesorption and readsorption of ligands during the process of aggregation may be involved in the effect.

A similar mechanism involving aggregates of DDA-capped CdTe QDs might be involved in the PL enhancement effect observed for dispersions of these particles. In a concentrated dispersion, several QDs may cluster together into an aggregate of colloidal NCs, quenching the PL. After dilution there will be more free solvent available for each NC, causing the hypothetical aggregates to disband. Since clustering facilitates energy transfer from smaller QDs with a wider bandgap to larger QDs with a more narrow bandgap, one would expect a consistent blueshift in the PL spectra if aggregates were indeed breaking apart. Figure 4.4 shows that this is not the case.

Additional evidence is found in DLS results obtained after dilution of crude Ar2 reaction mixture in toluene by a factor 100. By fitting DLS data, the hydrodynamic diameter of the particles in the colloidal dispersion can be inferred. Included in this measure of size are the diameter of the NC's capping ligands and solvation layer. Using an estimated length of 4 nm for each DDA molecule on both sides of the crystal, 3 nm for the NC itself, and 1 nm for toluene, the hydrodynamic diameter for a single particle should be approximately 13 nm.

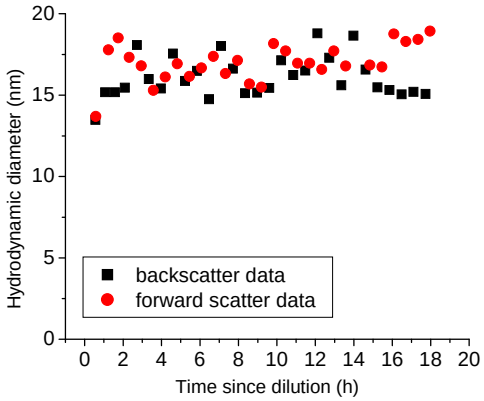

Figure 4.10: *Fit results of DLS experiments with freshly made dispersions of crude Ar2 CdTe reaction mixture in toluene (1:100) show that the hydrodynamic diameter of the colloids remains constant over time. The average of 16 nm is a typical hydrodynamic diameter for a single, unclustered TOP/DDA-capped CdTe NC.*

Indeed, figure 4.10 shows that this is the case. At all times, the average diameter seems to fluctuate around 16 nm. The small difference between the estimate and measurement arises in part from estimation uncertainty, in part from incongruence between the model's assumptions of a spherical particle and the real NC shape, and in part from experimental bias due to the fact that larger NCs in the ensemble contribute more strongly to the DLS signal than smaller ones.

Nonetheless, the results present strong evidence against the hypothesis that dilution of the QDs causes colloidal clusters to fall apart. Indeed, if any change to the hydrodynamic radius occurs after dispersion, it is an increase rather than a decrease. The first data point was taken approximately 30 minutes after dilution. There seems to be some increase in the hydrodynamic radius over the subsequent hour, so it may be interesting to repeat the experiment from an earlier starting point.

4.2.4 Relevance of a shift in the ligand adsorption equilibrium

Munro et al. have argued that changes in the ligand adsorption equilibrium should decrease the PL QY, as some ligands desorb and thereby increasing the amount of unbound states on the inorganic surface. [8] Although this can be expected for our samples as well, the mere unbinding of amine ligands should occur on a timescale of seconds or less. [24, 25] Therefore, by itself ligand desorption cannot fully explain the observed changes over the course of many hours. Furthermore, desorption of ligands is expected to decrease, not increase the PL QY, except perhaps for overloaded surfaces. This will be discussed in section 4.3.3.

Results from FTIR spectroscopy to be presented in paragraph 4.4 show that the amount of DDA on the surface stays essentially constant for CdTe QDs diluted in dodecane, although this may not be true for dispersions in the more polar toluene. More concrete evidence is given in section 4.3.5, where it is shown that PL enhancement also occurs after diluting CdTe QDs in 2 M DDA with a 2 M solution of DDA in toluene. The possible relevance of dilution will be further discussed in section 4.5.4.

4.2.5 Conclusions on potential mechanisms for PL enhancement

On the basis of optical spectroscopy and DLS measurements, several hypotheses commonly offered for PL enhancement have been evaluated for their bearing on the observed enhancement for both dark and illuminated DDA-capped CdTe QDs in an inert atmosphere.

The potential effect of solvent impurities is acknowledged, but it is experimentally verified that this would likely lead to PL quenching rather than enhancement. Furthermore, solvent impurities cannot account for the differences in the temporal evolution of CdTe QDs capped with different concentrations of DDA and ODA to be presented in paragraph 4.3.

The possibility of a decrease in reabsorption of emitted light is acknowledged but cannot account for the PL enhancement observed on the timescale of hours. Secondly, no reversal of redshift is found in emission spectra.

The possibility of a decrease in NC aggregation is ruled out because no reversal of redshift is observed in emission spectra, and no decrease in the hydrodynamic radius is found with DLS.

The relevance of a shift in the ligand adsorption equilibrium after dilution is acknowledged, but cannot by itself account for the long timescale on which PL enhancement is observed.

4.3 Role of the capping layer in PL evolution

Because the PL is highly dependent on the NC surface structure, changes in PL properties are often interpreted to track processes at the NC surface-ligand interface such as surface reconstruction. A detailed theoretical description of such processes is given in sections 2.2.4 and 2.2.5. In order to understand the role of the NC surface-ligand interface in the observed evolution of PL properties, experiments were performed with washed and recapped Ar2 CdTe QDs as simple model systems of which the NC surface is capped with only one type of ligand. In this way, the difference in temporal PL evolution for DDA- and ODA capped CdTe was investigated.

Table 4.2 lists all of the samples, which were prepared according to the procedure described in section 3.1.3. Of each sample a dispersion in toluene (1:100) was made, from which a small volume (3 mL) was taken to be illuminated for 1 second every 5 minutes whereas the rest was kept dark, each portion being discarded after use for a single measurement. More detailed descriptions of these PL measurements have been given in sections 4.1.2 and 4.1.3 for the dark and illuminated Ar2/2 M DDA dispersions, respectively. Several frames of the PL series for this sample are shown in figures 4.4a (illuminated sample) and 4.6 (dark sample).

Table 4.2: *Properties of washed and recapped Ar2 CdTe QD samples, as derived from absorption and PL spectra of 1:100 dispersions in toluene. The listed concentrations apply to the washed and recapped product prior to dilution.*

CdTe QD sample	**[QD] (mM)**	**Absorption maximum (nm / eV)**		**Initial excitonic emission maximum (nm / eV)**		**QD diameter (nm)**	**Initial PL QY**
Ar2/0.6 M DDA	0.22	536	2.31	561.2	2.209	3.0	0.16
Ar2/0.6 M ODA	0.22	535	2.32	562.2	2.205	2.9	0.12
Ar2/2 M DDA	0.17	535	2.32	558.7	2.219	2.9	0.19
Ar2/2 M ODA	0.14	533	2.33	557.2	2.225	2.9	0.17
Ar2/4 M DDA	0.02	531	2.33	553.7	2.239	2.9	0.21
Ar2/4 M ODA	0.02[7]			558.4	2.220		0.21[7]
Ar2/2 M DDA + 100 TDPA/QD	0.17	537	2.31	559.7	2.215	3.0	0.11

[7] No absorption spectrum was recorded for the Ar2/4 M ODA sample, but [QD] is equal to that of Ar2/4 M DDA, as these two samples were prepared in an identical way as described in section 3.1.3. In order to calculate the PL QYs, the absorbance at 400 nm was estimated to equal that of Ar2/4 M DDA.

4.3.1 Evolution of PL in dispersions of 2 M DDA/ODA CdTe QDs

We first present the results for dilutions of 2 M DDA and ODA samples, since these amine concentrations are similar to those in the crude reaction mixture and were used in the experiments discussed so far. Figures 4.11a and b show that the starting QY for ODA-capped dots was lower, so that there was more potential for improvement in these samples. In spite of this, periodically irradiated dispersions of CdTe QDs with ODA-capping brightened less than their DDA-capped counterparts, providing a first indication that the observed enhancement is ligand-dependent.

A more striking difference is the behavior of dots kept in the dark: whereas dispersions of DDA-capped dots showed just slightly less PL enhancement when deprived from light, the QY of dark dispersions with ODA surfactants increased from 17% to no more than 18% in 2 hours and subsequently declined. Figure 4.11d shows that this quenching was accompanied by a blueshift of the PL, suggesting a process that reduces the size of the dark ODA-capped NCs, such as partial dissolution. For the other three dispersions, figures 4.11c and d show a correlation between rapid PL enhancement and a redshift of the exciton emission in the first 5 to 10 hours. With DDA-capped dots, the redshift is more pronounced when they are kept dark.

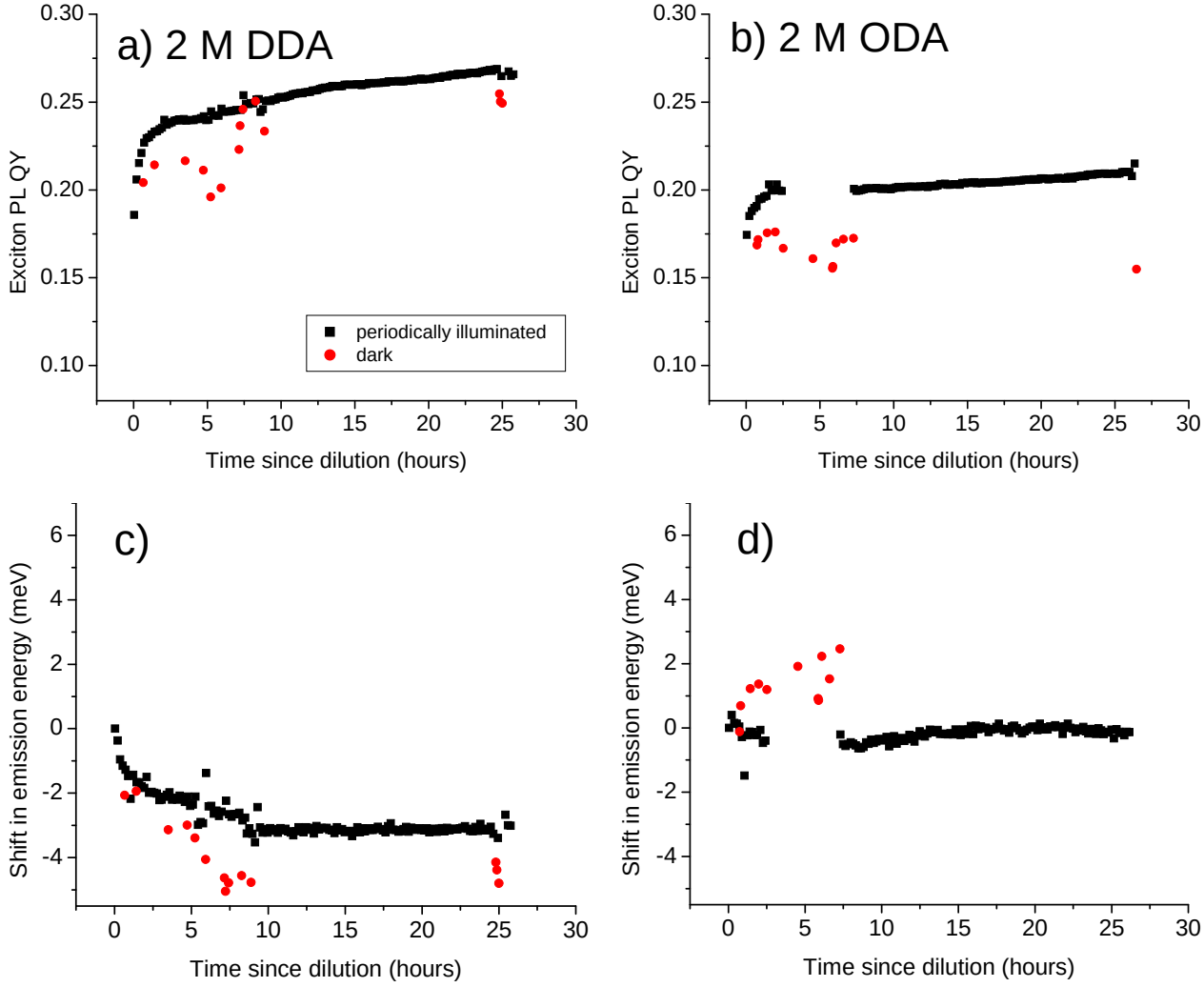

Figure 4.11: *Temporal evolution of the exciton PL QY and emission energy of washed Ar2 CdTe QDs recapped in 2 M DDA* ***(a,c)*** *and ODA* ***(b,d)*** *and diluted in toluene (1:100). For each data point in the dark series, a new portion of dispersion was used that had been shielded from light since dilution. Illuminated samples were exposed to a brief flash of 400 nm light every 5 minutes.*

It is also noted that the DDA-capped dots seemed to show much more sensitivity to irradiation with 400 nm light than the ODA-capped dots. This is not only visible in the QY evolution of illuminated samples, but also in the large error for light-shielded dispersions with DDA surfactants. This error exceeds the 5% uncertainty with which the PL of Rhodamine B was measured (figure 4.4b), indicating that sample-specific properties are involved rather than general problems with the measurement setup. It seems likely that the dark QDs were strongly affected by the 1 s exposure to light that was necessary to record a PL spectrum. Since a new portion of dark dispersion was used for each data point in the dark series, these errors did not accumulate. Rather, small fluctuations in the duration and intensity of the flashes due to limitations of equipment lead to relatively large random errors in both directions.[8]

If indeed one flash of the LED is sufficient to make "dark" CdTe/DDA dots behave similarily to their more often illuminated counterparts, future experiments should use a lower LED intensity to observe more pronounced differences between dark and illuminated dispersions. On the other hand, the CdTe/ODA dots might not have shown any enhancement at all, had they been illuminated with a lower LED intensity[9]. These dots showed much less sensitivity to irradiation, which is presented as further evidence that ligands are involved in the enhancement processes.

In conclusion, the results so far favour the hypothesis that the observed evolution of PL properties in amine-capped CdTe QDs is related to processes at the NC surface-ligand interface, both when illumination is involved and when it is not. Furthermore, the difference between illuminated and dark samples suggest that an activation energy is involved, which is higher for ODA-capped than for DDA-capped CdTe QDs.

4.3.2 Evolution of PL in dispersions of 0.6 M DDA/ODA CdTe QDs

Figure 4.12 shows how the PL of CdTe QDs in 0.6 M DDA or ODA evolved from the moment they were diluted in toluene. Notice that the axes are drawn to the same scale as those in figure 4.11, highlighting the subtlety of the changes in QY as well as the significance of the changes in the exciton peak position for the 0.6 M samples.

The initial QY for the DDA-stabilized sample was only slightly lower than that of Ar2/2 M DDA, whereas the surface of the ODA-capped dots was apparently damaged during recapping as evidenced by a low initial QY. Both populations of QDs seem to have started out with a decline in QY after dispersion in toluene, which was arrested in the following 2 to 3 hours for the samples under light. A subsequent recovery process was recorded for the 0.6 M ODA sample., although after 18 hours its QY had still not reached the lowest value measured for the DDA-capped samples. The dark ODA-stabilized dispersion stayed at a minimum QY, indicating that the recovery path was photo-activated. A similar photo-activated recovery process seems to be at play for the illuminated Ar2/0.6 M DDA dispersion. This is supported by the chance observation of a sudden drop in the QY evolution curve, when after 1.5 hours one flash of periodic illumination was accidentally delivered 4 minutes later than it should have been.

---

[8] An additional explanation may be found in environmental light: although experiments were carried out in a dark room and a dark glovebox, diffuse light from a CRT computer monitor was used to work in the glovebox. When transfering a dark sample from its container to the sample holder of the spectrometer, it was exposed to this environmental light for approximately 20 seconds. Variations in the duration of this exposure, as well as the intensity of the CRT light, are expected to partially account for the large error in the Ar2/2 M DDA dark series.

[9] Although the 2 M ODA data in figures 4.11b and d is interrupted between 2.5 and 7 hours, periodic illumination was continued in this period of time. Thus, the illuminated ODA-capped dots received equal doses of radiation as the DDA-capped dots. The collected spectra could not be used because of instability in the signal observed by the CCD, including that of the dye standard. The signal was restabilized 7 hours into the measurement.

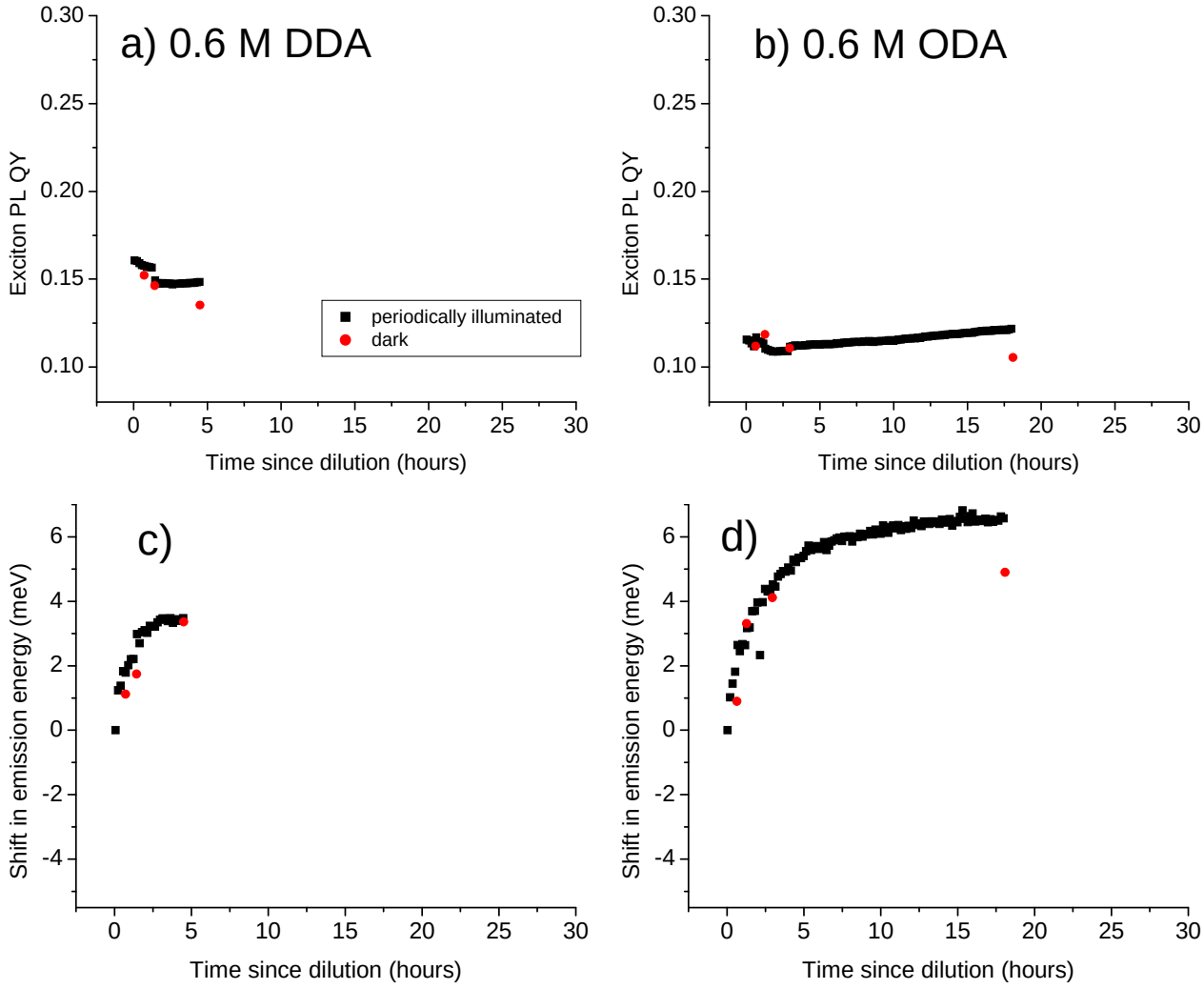

Figure 4.12: *Temporal evolution of the exciton PL QY and emission energy of washed Ar2 CdTe QDs recapped in 0.6M DDA* ***(a,c)*** *and ODA* ***(b,d)*** *and diluted in toluene (1:100). For each data point in the dark series, a new portion of dispersion was used that had been shielded from light since dilution. Illuminated samples were exposed to a brief flash of 400 nm light every 5 minutes.*

For all samples, the initial quenching of PL was accompanied by a gradually converging blueshift. This can be understood as a recovery from effects during or after washing and recapping, because the initial position of the exciton peak was significantly redshifted in these samples as listed in table 4.2. Possibly, processes at play since the dots were washed competed with processes that gained momentum after dispersion in toluene and illumination. The blueshift could indicate dissolution of the QDs, disbanding of aggregates that had formed due to a lack of colloidal stabilization, or thermally activated escape of weakly bound inorganic atoms from the crystal.

In conclusion, the results show quenching of the PL of Ar2 CdTe QDs recapped in 0.6 M DDA or ODA. This indicates that the surface of the QDs is insufficiently passivated after dispersion in toluene. No trends similar to the PL enhancement of fresh Ar2/2 M DDA or ODA were observed. However, PL quenching could be partially reversed by a photo-activated process. Possible mechanisms for this process include photo-annealing and reconstruction of the surface induced by local heating of the surfactant shell, as will be discussed in paragraph 4.5.3. Some support for the former mechanism is found in the resemblance of the Ar2/0.6 M ODA QY evolution to that of the aged dispersion in figure 4.7.

4.3.3 Evolution of PL in dispersions of 4 M DDA/ODA CdTe QDs

Figure 4.13 shows how the PL of CdTe QDs in 4 M DDA or ODA evolved from the moment they were dispersed in toluene. Note that the concentrations of amine used for recapping of these samples prior to dispersion in toluene are equivalent to using pure DDA or ODA as solvent. In general, the results depict similar trends for DDA and ODA capped dispersions, suggesting that the superabundance of ligands overrules the possible effect of the length of the ligand alkyl chain on the NC surface structure.

The initial QYs for these dispersions were by far the highest in the reported series of experiments with Ar2 CdTe QDs. This cannot be directly correlated to the higher concentration of ligands in comparison to the other samples, because the concentration of QDs also differed. As listed in table 4.2, all stock solutions contained ~ 0.2 mM QDs, except for the 4 M DDA/ODA stocks which contained only 0.02 mM QDs. This stock solution was dispersed in toluene at an unchanged 1:100 ratio. This means that the amount of ligands per QD is 20 times higher in these samples than in 2 M DDA/ODA.

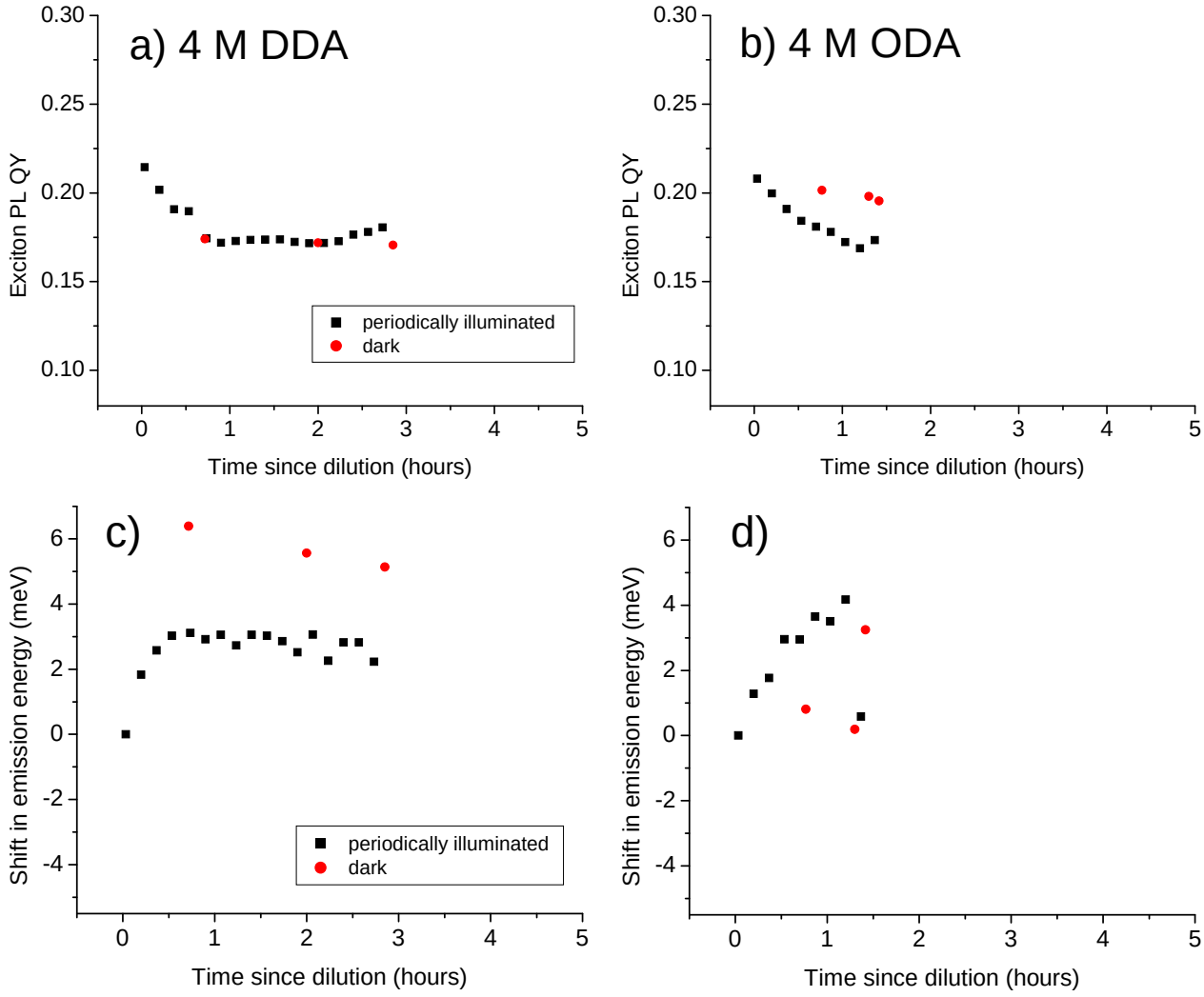

Figure 4.13: *Temporal evolution of the exciton PL QY and emission energy of washed Ar2 CdTe QDs recapped in 4 M DDA* ***(a,c)*** *and ODA* ***(b,d)*** *and diluted in toluene (1:100). For each data point in the dark series, a new portion of dispersion was used that had been shielded from light since dilution. Illuminated samples were exposed to a brief flash of 400 nm light every 5 minutes.*

In the first hour after dispersion of the Ar2/4 M DDA QDs in toluene, a rapid decline of the QY was measured. This decline followed roughly the same trend for illuminated and dark DDA-capped CdTe (figure 4.13a), although clear differences in the peak position (figure 4.13c) suggest that the similarity could be superficial. Following the decline was a period of stabilization and recovery, similar to that seen for dispersions of 0.6 M DDA/ODA (figures 4.12a and b) but on a larger scale. Unlike the 0.6 M samples, the quenching of 4 M samples did not appear to be inhibited by illumination. The QY evolution of ODA-capped QDs (figure 4.13b) followed the same overall trend as seen with 4 M DDA, but uniquely showed greater PL quenching for the dispersion that was illuminated than for the dark dispersion, although shifts in the exciton peak position were similar (figure 4.13d).

The exciton PL of all Ar2/4 M DDA and ODA dispersions shifted to the blue, as was also seen for dispersions of 0.6 M DDA/ODA in figures 4.12c and d. This could indicate partial dissolution of the QDs, disbanding of aggregates, or thermally activated escape of weakly bound inorganic atoms from the crystal. A likely explanation is the removal of inorganic atoms from the surface by desorbing ligands.

A possible explanation for the trend shown in figure 4.13a is as follows. Excessive capping of the NC surface blocks processes such as reconstruction, effectively locking the NC in its state. After dilution, DDA molecules desorb from the overloaded surface until a new equilibrium is reached. The sudden efflux of ligands causes an initial quenching of the PL QY, but as it unlocks the surface to reconstruction processes, this trend is progressively ameliorated. Indeed, a beginning enhancement can be discerned after 2 hours. The proposed mechanism predicts a continuation of this trend. If the enhancement occurs by the same mechanism as shown in figure 4.11a, it will be accompanied by a redshift of the exciton emission peak similar to that shown in figure 4.11c.

In conclusion, the results indicate that the surface of Ar2 CdTe QDs recapped in 4 M DDA or ODA is initially well-passivated. After dispersion in toluene, PL quenching and a blueshift are observed.. Whether this is a consequence of dilution cannot be inferred from the current data, so that the possibility cannot be excluded that part of the processes involved in the observed quenching already took place in the undiluted sample. However, under the assumption that the PL evolution observed in the first hour after dilution is predominantly due to desorption of ligands, a mechanism for the observed changes is presented that predicts PL enhancement and a redshift after the initial quenching and blueshift.

4.3.4 Evolution of PL in a dispersion of 2 M DDA CdTe QDs with 100 TDPA/QD

Figure 4.14 shows data from one of two experiments designed to gain insight in the involvement of DDA with the PL enhancement observed after dilution of CdTe/2 M DDA QDs. The reference experiment documenting this effect (figure 4.11a) was repeated with a sample laced with a small amount of *n*-Tetradecylphosphonic acid (TDPA), equivalent to 100 molecules per QD. Due to the strong affinity of its head group for the NC surface, TDPA is expected to displace DDA at several adsorption sites and thus interact with the mechanism of PL enhancement, i.e. surface reconstruction. Whereas DDA has a high exchange rate due to its relatively weak bond with the surface [24, 25], TDPA binds strongly and is thus presumed to be a less dynamic ligand.

The results show that illuminated dispersions of CdTe/2 M DDA+TDPA evolve in a way similar to the CdTe/2 M DDA reference. However, only the dispersion free of TDPA shows PL enhancement in the dark. This indicates that partial replacement of the DDA capping layer with TDPA introduces a requirement of photo-activation. This can be understood as TDPA ligands increasing the activation energy barrier for surface reconstruction, which is in agreement with the more rigid, less dynamic nature of their adsorption to the surface. This again highlights the active role of the capping layer in surface reconstruction.

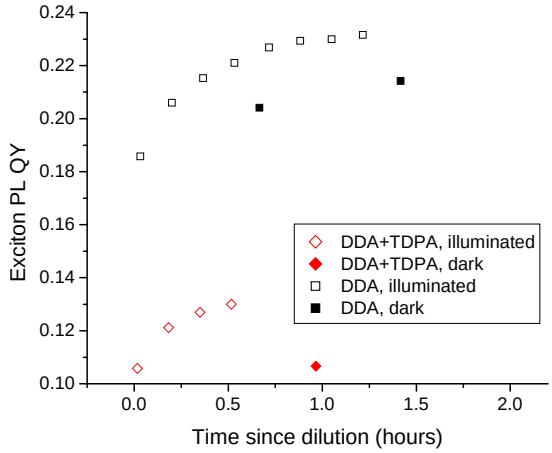

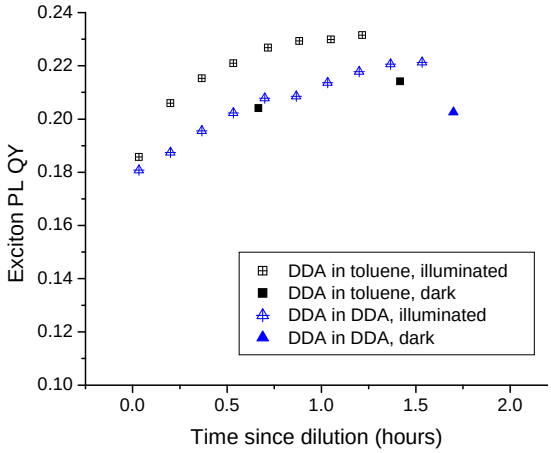

Figure 4.14 (left): *Temporal evolution of the exciton PL QY of washed CdTe QDs recapped in 2M DDA with 100 TDPA/QD, after dispersion in toluene (1:100). Data of the TDPA-free experiment from figure 4.11a is included as a reference.*

Figure 4.15 (right): *Temporal evolution of the exciton PL QY of washed CdTe QDs recapped in 2M DDA and diluted (1:100) in a mixture of 2 M DDA and toluene. Data of the experiment from figure 4.11a using toluene as solvent is included as a reference.*

4.3.5 Evolution of PL in a dispersion of 2 M DDA CdTe QDs with constant [DDA]

A second experiment was performed to provide insight in the involvement of DDA with the PL enhancement observed after dilution of CdTe/2 M DDA QDs. The reference experiment documenting this effect (figure 4.11a) was repeated, replacing pure toluene with a mixture of DDA and toluene as solvent. The concentration of the DDA in this mixture was made to match that.of the recapping solution, i.e. 2 M, so that the QDs experienced no change in [DDA] upon dilution.

The results given in figure 4.15 confirm that enhancement of the PL takes place after CdTe/2 M DDA QDs are diluted in 2 M DDA, albeit at a slower rate than for dilutions of the same NCs in toluene. In the first 90 minutes the illuminated dilution in toluene/DDA seems to brighten at a comparable rate to the dark dilution in toluene. Even without illumination, the dark QDs dispersed in toluene/DDA still show an increase in QY from 18% to 20% after 1.7 hours.

The results demonstrate that triggering of PL enhancement is not contingent on changes in the DDA concentration. This introduces the question whether the reduction in [QD] is a trigger. This is not necessarily so. It is possible that not one, but several combinations of changes in the [DDA]/[QD] ratio, the [DDA]/[toluene] ratio and the [QD]/[toluene] ratio trigger the effect.[10] It is also possible that concentration changes are not triggers for the enhancement effect at all. This will be discussed in section 4.5.4.

[10] New clues could be obtained from an investigation on the PL evolution of a dispersion in which [DDA] is reduced, while [QD] remains constant. This could for example be done by 'diluting' a mixture of QDs with a solution that has the same concentration of QDs, but is poor in surfactants. However, the QDs in the former mixture would have a different surface structure than those in the latter. For this reason a different protocol should be devised.

4.3.6 Conclusions on the role of the capping layer in PL evolution

The striking difference between the PL evolution of ODA- and DDA-capped CdTe QDs kept in the dark confirms that the PL enhancement observed for DDA-capped dots is a consequence of ligand-dependent surface reconstruction.

For ODA-capped and DDA/TDPA-capped CdTe QDs, energy barriers for surface reconstruction of at least 26 and at most 3100 meV[11] are identified by differences in the PL evolution of dark and illuminated dispersions. Energy barriers for DDA-capped CdTe QDs are estimated at the order of kT, as dispersions of these NCs show evidence of surface reconstruction without being illuminated and increasingly so when illuminated.

The PL increase for DDA-capped CdTe QDs was shown not to be contingent on changes in the DDA concentration, as it was observed in dispersions with [DDA] equal to the stock.

[11] The lower bound is given by the thermal energy at room temperature, kT = 26 meV. The upper bound is given by the 400 nm excitation light, hc / λ = 3100 meV. It is assumed that absorption of a single photon can activate reconstruction, because the light intensities were too low for significant 2-photon excitation to occur.

4.4 DDA ligands probed by FTIR spectroscopy

4.4.1 Identifying vibrations for free and bound ligands

Capping ligands are a likely mediator through which changes in the surface structure can affect the PL, since they play a crucial role in facilitating or blocking reconstruction of the NC surface as described in section 2.2.5. Fourier transform infrared spectroscopy (FTIR) provides a good way to investigate the binding of amine ligands to colloidal QDs dispersed in a solvent. Especially informative is the NH scissoring peak appearing around 1620 cm^{-1} for free amines, as this peak splits in two when they bind to a CdSe or CdTe surface. [38] For ODA-capped CdSe, a split to 1544 and 1635 cm^{-1} is reported in literature; with DDA-capped CdTe, we found peaks at 1568 and 1650 cm^{-1}.

Unfortunately, it is difficult to resolve these peaks when using toluene as a solvent, as it often saturates the signal near these energies. For this reason, dodecane was used instead. PL enhancement similar to that in toluene was measured for dispersions of DDA-capped CdTe in dodecane; these results are presented in the appendix. In this solvent, addition of DDA was required to prevent the QDs from aggregating, presumably because DDA has relatively less affinity for the QD surface in dodecane than it has in toluene.

Figure 4.16a shows the FTIR spectra of washed WA2 QDs in dodecane with increasing amounts of DDA added. The concentration of QDs in these samples is 16 µM, as determined by absorption spectra included in the appendix. Besides the IR absorption peaks at 1618 and 1667 cm^{-1} (corresponding to NH scissoring modes), energies of interest are 1073 cm^{-1} (C-N stretching) and 721 cm^{-1} (backbone C-H rocking). The latter peak includes a large contribution by dodecane, whose C-H rocking vibration is at nearly the same energy. Figure 4.16b shows how the absorbance of the NH scissoring peaks increases with the amount of DDA added to the QD dispersion.

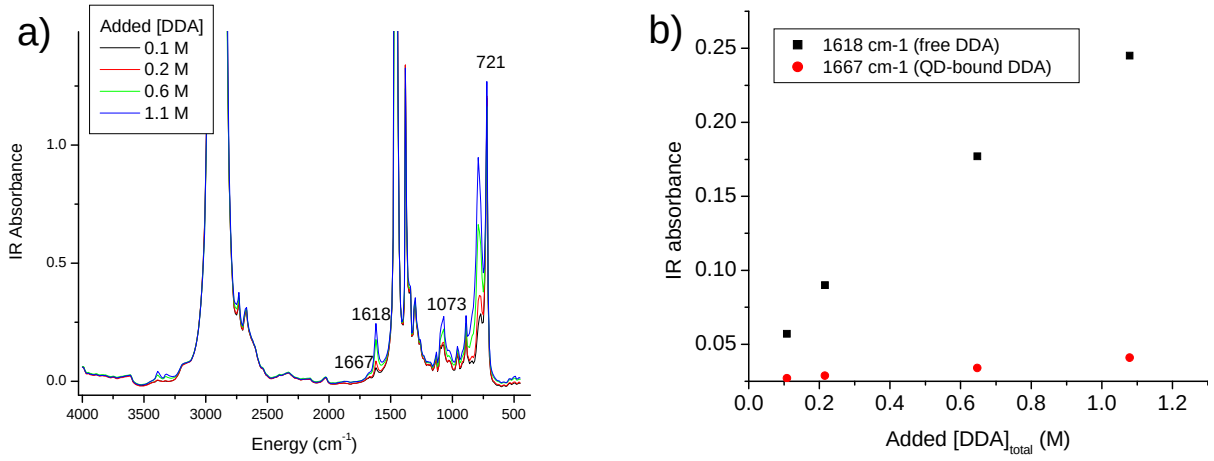

Figure 4.16: (a) *FTIR spectra of washed WA2 CdTe QDs in dodecane with increasing amounts of DDA added.* ***(b)*** *the absorbance of the NH scissoring peaks increases as DDA is added.*

4.4.2 Evolution of amine NH scissoring vibrations

By following the NH scissoring peaks as a function of time after dilution, the ratio between bound and free amine ligands can be tracked. Figure 4.17 shows that both absorbances remain essentially constant, leading to the conclusion that no changes in quantitative surface coverage seem to occur in the first 40 minutes after dilution in dodecane. Ligands may be involved in the PL enhancement by redistribution over the surface, but the net amount seems to stay constant. This is in agreement with the PL experiment discussed in section 4.3.5, which demonstrated that the PL enhancement process can be triggered without changes in the DDA concentration of the solution.

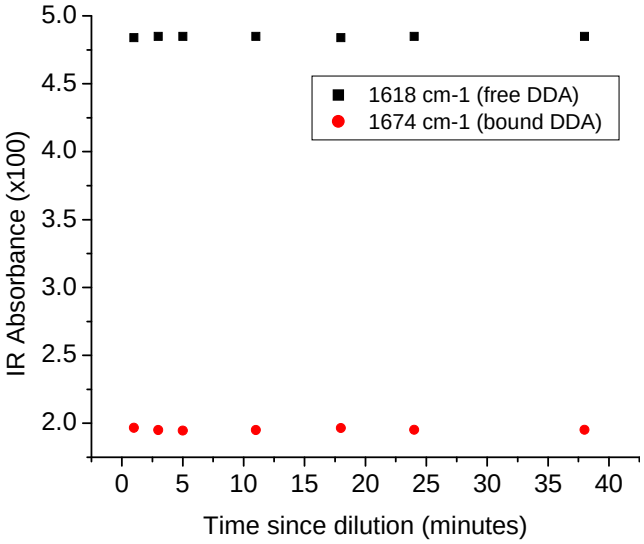

Figure 4.17: *Temporal evolution of IR absorbance at 1618 and 1674 cm^{-1} for a freshly diluted dispersion of DDA-capped CdTe QDs in dodecane.*

Despite this, FTIR results for colloidal dispersions in dodecane cannot be easily extrapolated to dispersions in the more polar toluene. For colloidal QDs in such polar solvents, evidence from PL measurements for desorption of amine ligands has been reported. [20]. It would thus be instructive to repeat these FTIR measurements in a more polar solvent and compare the evolution of the 1618 and 1674 cm^{-1} vibrations to figure 4.17.

4.4.3 Evolution of carbon chain CH rocking vibration

Although no changes were observed in the NH scissoring vibrations of DDA after dilution of DDA-capped CdTe QDs in dodecane, the backbone C-H rocking mode at 721 cm^{-1} did change over time. Figure 4.18 shows that the peak both decreased in intensity and shifted to a slightly lower energy. Figure 4.19 shows that both changes follow the same trend. This may be explained by considering that the peak is actually a convolution of two peaks, the C-H rocking mode of DDA and that of dodecane. Due to the head group of DDA, the energy of this mode differs slightly from that in dodecane. The shift in the peak maximum likely indicates that only one of the two peaks is actually decreasing in intensity. From the current data it cannot be determined if this peak corresponds to DDA or to dodecane.

Note that the changes in the C-H rocking mode occur rapidly in the first hour after dilution, similarly to the initial rise of the PL enhancement described in section 4.3.1 for figure 4.11. This correlation suggests that the alkyl chain of DDA has an active role in the reconstruction of the surface. A possible explanation for the reduced vibrational intensity is that DDA ligands form more linear, monolayer-like structures on the newly reconstructed surface.

The results suggest that the alkyl chain vibration at 721 cm^{-1} may be more relevant to the reported surface reconstruction of DDA-capped CdTe QDs than the 1618 and 1674 cm^{-1} vibrations. This means that it will be useful to repeat these experiments with toluene as a solvent. Although the peaks around 1650 cm^{-1} will likely be obscured, toluene has no strong bands near 721 cm^{-1}, allowing any changes in the C-H rocking mode vibration of DDA to be unambiguously observed.

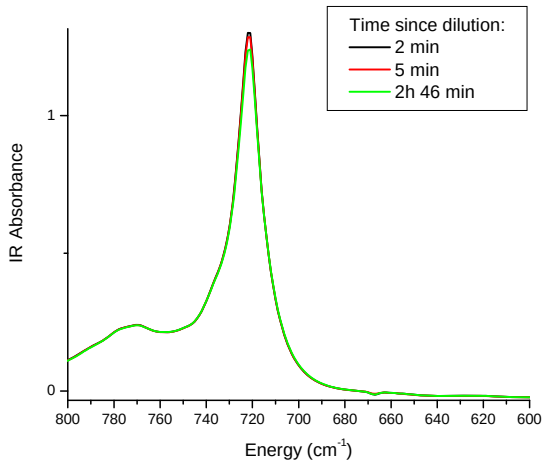

Figure 4.18: *The IR absorbance peak at 721 cm^{-1} at 2, 5 and 146 minutes after dilution.*

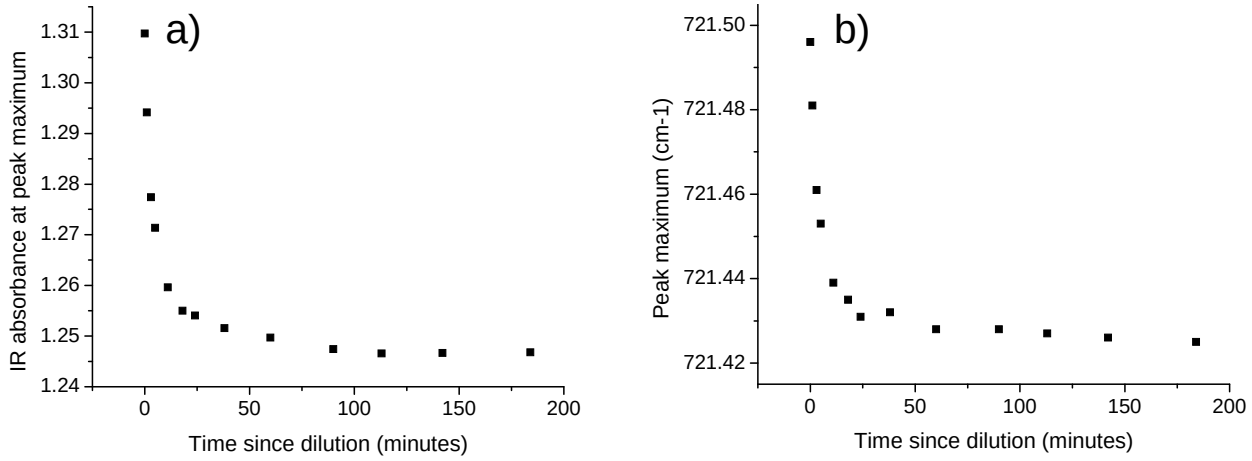

Figure 4.19: *Temporal evolution of (a) IR absorbance and (b) peak position for the rocking vibration of a freshly diluted dispersion of DDA-capped CdTe QDs in dodecane.*

4.5 Proposed model of ligand-mediated surface reconstruction

4.5.1 Original cause for PL enhancement

The ultimate cause of PL enhancement is an incongruence between the initial state of the NC-ligand system and equilibrium state(s) of lower free energy available for that particular system. Such a distance in the free energy landscape is created by chemical events in the history of the NC such as synthesis, washing and recapping. These events create energy levels in the bandgap through which an exciton can decay non-radiatively. Reconstruction of the NC surface is required to passivate these quenching surface states. [39]

The temporal evolution of the PL can then be understood as a set of footprints left by the NC travelling over the free energy landscape towards a deeper minimum. Different footprints may be found, depending on the path that is travelled – that is, the mechanism by which free energy is minimized. The endpoint may also differ, because energy barriers or "bears on the road" can prevent the system from reaching the global minimum. Instead, the system will relax into a local minimum.

In this paragraph, the observed footprints are used to trace the pathways of the several different colloidal amine-capped CdTe QDs that were studied. Specifically, the role of the ligands is discussed.

4.5.2 Origin of energy barriers

The reported PL experiments indicate that the activation energy for surface reconstruction is larger for a surface capped with longer-chained primary amines. This is explained by the larger van der Waals interactions between the alkyl chains of these ligands. Surface reconstruction involves motion of inorganic atoms over the surface. Such motion is mediated by the presence of capping ligands on the atoms, since these ligands must either detach or move along with the inorganic atom. Depending on the configuration of the capping layer, this will involve some degree of temporary loss in van der Waals interactions between neighbouring ligands, thus introducing a conflict between the minimization of free energy for ligands and for the inorganic surface.

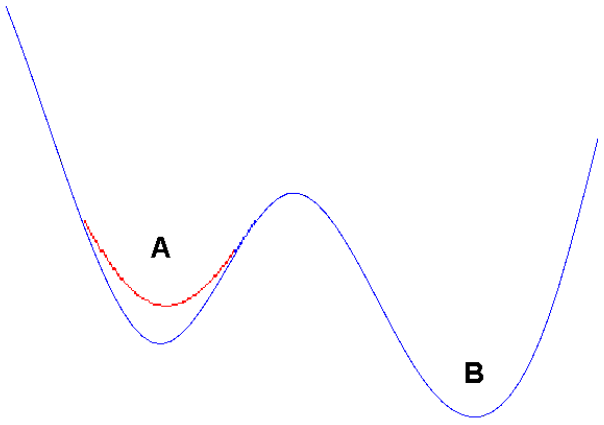

Figure 4.20: *A simplified model free energy function to illustrate the relation between the surfactant alkyl chain length and the activation energy for surface reconstruction. In the metastable state A, the ligands impose a structure on the NC surface to maximize van der Waals interactions between ligand alkyl chains. These interactions are stronger in the free energy function of QDs capped with ODA (blue line) than for DDA (red line). Input of sufficient activation energy will allow reconstruction of the surface-ligand system to state B, in which the free energy of the inorganic crystal is minimized at some expense of the interactions between ligands.*

State A in figure 4.20 represents the state in which the surface is ordered in such a way that the free energy of ligands is minimized. This might involve one surface Cd site being bound by two amine ligands, or by none at all depending on the location of the site and the opportunities this offers for ligands to minimize the free energy of their

alkyl chains. Because of this, there will be quenching states in the band gap of the inorganic crystal, keeping the QY low. In state B, the free energy of the NC surface is minimized. The configuration of the ligands is subordinate to the inorganic structure, so that optimal passivation is reached. In this state, the PL QY will be high. Instead of van der Waals interactions between ligand tails, the interactions between ligand head groups and the inorganic crystal will be maximized.

Note that figure 4.20 is a simplified model of reality: for an actual QD, the free energy function is multidimensional and will likely have multiple metastable states. It might also be possible that a ligand-imposed surface structure is the more favourable state, reversing the labels A and B.

4.5.3 Ligand-mediated surface reconstruction

Surface reconstruction is depicted in figure 4.20 as the transition from state A to state B. This requires the capping layer to temporarily be dynamic enough to facilitate the coordinated motion of atoms over the surface. For this reason, the system will be kinetically trapped in state A until sufficient activation energy is introduced. The longer the alkyl chains of the ligands are, the deeper state A will be and the more rigid, solid-like the configuration of the capping layer will be. This is observed for ODA-capped CdTe QDs, which show enhancement of the PL after being illuminated or heated [11] but not in the dark at room temperature.

When energy is supplied to a QD in state A, the increased mobility of ligands allows reconstruction of the NC surface-ligand interface. The surfactants and inorganic atoms move around the surface until the equilibrium state B is reached in which the NC has the most favourable shape. The redshift observed for samples that showed PL enhancement can be understood as a result of such shape changes.

Although ligands will be highly dynamic during the transition from state A to B, in the final equilibrium state the bonds between ligand headgroups and inorganic surface atoms are maximized, which will attenuate the mobility of the attached ligands. DDA ligands form more linear, monolayer-like structures on the newly reconstructed surface. The decreasing C-H vibration of the alkyl chains depicted in figure 4.19 can be seen in this light.

Instead of through illumination, the energy for reconstruction may also be supplied in the form of direct thermal heat, in which case the provided model gives a free-energy interpretation of luminescence temperature antiquenching (LTAQ). An essential difference between illumination and thermal heating lies in the selectiveness of the former. QDs in which the exciton decays non-radiatively will generate more heat than QDs that release most of the absorbed energy as light. Thus, QDs with quenching states are selectively heated upon illumination. Section 4.1.4 shows that there are only little changes in the PL decay curve of a sample in which the PL was enhanced after illumination, supporting this hypothesis. Unfortunately, no PL decay curves have been recorded for DDA-capped CdTe QDs in which PL is enhanced without illumination.

LMSR is expected to be of influence across a wide range of colloidal nanoparticles, although the combined properties of the < 3.0 nm DDA-capped CdTe QDs used in this work likely make it especially liable to the effect. Amine-capped CdSe QDs may be useful model systems for the study of the mechanism, as LTAQ has been reported for CdSe. Results in the appendix show strong enhancement for TOP/HDA-capped CdSe QDs freshly diluted and under illumination.

In conclusion, ligands are not bystanders or bears on the road, but co-travelers with the inorganic crystal on the free energy landscape. Thus, a more appropriate way to describe this landscape would be a free energy dance floor, on which some NC-ligand couples have the bad habit of wanting to go in different directions. External stimuli such as illumination may help resolve their conflict.

4.5.4 Effect of dilution on surface reconstruction

The experiments in this thesis show that surface reconstruction can be triggered by illumination. Although PL enhancement as a consequence of reconstruction is also observed for DDA-capped QDs that are not illuminated, it remains unclear whether this is triggered by dilution or was already taking place in the concentrated solution. The direct consequences of dilution include exposure of the CdTe QDs to sudden changes in the [DDA]/[QD], [DDA]/[toluene] and/or [QD]/[toluene] ratios, as well as increased transparancy of the QD solution to light.

The only direct experimental evidence available is discussed in section 4.3.5, where it was shown that changes in the DDA concentration are not required to trigger PL enhancement, but they do appear to somewhat accelerate it.

Although it is recognized that the surface of colloidal nanoparticles continues to reconstruct for several days after synthesis [8, 20, 21], the QDs used in the Ar1 and WA2 measurements reported here were synthesized at least 6 months prior to measurement. If indeed there is still evolution of the surface on this timescale, then the rate of that evolution must be very small compared to the rate after dilution in toluene. For a typical dispersion diluted from crude reaction mixture, the PL QY increases from 14% to 20% in 12 hours (when illuminated)[12]. Clearly such a rate cannot be sustained for 6 months. Therefore, it seems that the surface reconstruction processes that lead to PL enhancement are greatly accelerated directly after dilution. This either means that the energy barrier to surface reconstruction is lowered at the moment of dilution, or some form of energy is supplied to the system at the moment of dilution, or both of these.

Alternatively, the faster PL evolution of illuminated dilutions compared to illuminated crude mixtures could be explained by the increased transparancy of a dilution. To verify this, a comparison should be made between the PL evolution of crude reaction mixture and a dilution, both stored in the dark.

It is likely that some evolution of the surface was taking place immediately prior to dilution in the Ar2 samples used for the experiments discussed in paragraph 4.3. These QDs were diluted in toluene directly after 12 hours of stirring in a concentrated ligand solution, as described in section 3.1.3. Although some equilibration of the surface following the washing and recapping process likely remained after 12 hours, figure 4.15 contains evidence that this occurred slowly, that is on relatively long timescales compared to the PL measurements performed. The PL series shown in figure 4.15 compare the dilution of Ar2/2 M DDA in toluene with the dilution of the same in 2 M DDA. The former experiment was performed immediately after recapping, whereas the latter was performed 10 days later. Still, there is a striking similarity between the initial QYs. The observation that hardly any changes occurred in the concentrated stock solution after 10 days, whereas diluted mixtures showed evolution on a timescale of hours, provides further support for the suggestion that dilution accelerates surface reconstruction of these samples in some way.

As mentioned in the discussion of FTIR results in section 4.3.2, when dispersing colloidal NCs in relatively polar solvents such as toluene ligands are reported to desorb. [20] This is detrimental to the PL QY if it leads to uncovered surface atoms, but for QDs with an initially overloaded surface such desorption may lead to PL enhancement. An example of such an effect may have been found in the results given in section 4.3.3 for Ar2 CdTe QDs recapped in 4 M DDA/ODA.

[12] Estimated using the PL series of freshly diluted Ar1 in figure 4.7, and its known QY of 14%, 3 minutes after dilution, which was measured with an integrating sphere setup. There is yet no reliable data on the enhancement for non-illuminated crude reaction mixture. Although this data is available for Ar2, that sample has been washed and recapped soon before the measurement.

5 Conclusions

For DDA- and ODA-capped CdTe QDs of diameter 2.7 to 2.9 nm in toluene, the temporal evolution of the PL is investigated. For both illuminated and dark DDA-capped QDs, enhancement of the PL QY accompanied by a redshift of the exciton peak position is found. The PL of ODA-capped QDs shows more moderate enhancement upon illumination and is quenched and blueshifted for samples shielded from light.

The observed enhancement cannot be accounted for by solvent impurities, a decrease in reabsorption, redispersion of aggregated NCs or shifts in the ligand adsorption equilibrium. The striking difference between the PL evolution of ODA- and DDA-capped CdTe QDs confirms that this evolution is a manifestation of processes at the NC surface-ligand interface. The differences are explained by the presence of ligand-imposed energy barriers on the order of kT and > kT for surface reconstruction of the DDA- and ODA-capped surfaces, respectively.

The PL increase for DDA-capped CdTe QDs is not contingent on a decrease in the DDA concentration by dilution. Furthermore, for DDA-capped CdTe in dodecane, the infrared absorption at energies related to the NH scissoring modes of surface-bound and free amines is found to remain constant in time after dilution. However, a decrease in the infrared absorption at the alkyl chain rocking vibration mode (721 cm^{-1}) is observed on the same timescale as the PL enhancement. It is concluded that the surface coverage with DDA changes qualitatively rather than quantitatively.

A model is proposed that explains this form of surface reconstruction as a transition from a state in which the rigid capping layer imposes disorder on the NC, to a state in which the NC dictates the configuration of the capping layer. It is suggested that illumination locally heats the capping layer of QDs in which the exciton decays non-radiatively, so that the effect is similar to earlier reports of luminescence temperature antiquenching in amine-capped CdSe QDs.

6 Bibliography

[1] J. P. Borel, "Thermodynamical size effect and the structure of metallic clusters," *Surface Science*, vol. 106, no. 1-3, pp. 1–9, 1981.

[2] L. B. Hunt, "Gold based glass and enamel colours," *Endeavour*, vol. 5, no. 2, pp. 61–67, 1981.

[3] K. Kordás, G. Tóth, P. Moilanen, M. Kumpumäki, J. Vähäkangas, A. Uusimäki, R. Vajtai, and P. M. Ajayan, "Chip cooling with integrated carbon nanotube microfin architectures," *Applied Physics Letters*, vol. 90, no. 12, p. art. 123105, 2007.

[4] M. A. Shannon, P. W. Bohn, M. Elimelech, J. G. Georgiadis, B. J. Marias, and A. M. Mayes, "Science and technology for water purification in the coming decades," *Nature*, vol. 452, no. 7185, pp. 301–310, 2008.

[5] L. E. Brus, "Electron-electron and electron-hole interactions in small semiconductor crystallites: The size dependence of the lowest excited electronic state," *The Journal of chemical physics*, vol. 80, no. 9, pp. 4403–4409, 1984.

[6] W. C. W. Chan, D. J. Maxwell, X. Gao, R. E. Bailey, M. Han, and S. Nie, "Luminescent quantum dots for multiplexed biological detection and imaging," *Current opinion in biotechnology*, vol. 13, no. 1, pp. 40–46, 2002.

[7] G. Kalyuzhny and R. W. Murray, "Ligand effects on optical properties of CdSe nanocrystals." *The journal of physical chemistry. B*, vol. 109, no. 15, pp. 7012–21, Apr. 2005.

[8] A. Munro, I.-L. Plante, M. Ng, and D. Ginger, "Quantitative study of the effects of surface ligand concentration on cdse nanocrystal photoluminescence," *Journal of Physical Chemistry C*, vol. 111, no. 17, pp. 6220–6227, 2007.

[9] N. Yaacobi-Gross, M. Soreni-Harari, M. Zimin, S. Kababya, A. Schmidt, and N. Tessler, "Molecular control of quantum-dot internal electric field and its application to CdSe-based solar cells." *Nature materials*, vol. 10, no. 12, pp. 974–9, Dec. 2011.

[10] S. F. Wuister, C. De Mello Donega´, and A. Meijerink, "Influence of thiol capping on the exciton luminescence and decay kinetics of cdte and cdse quantum dots," *Journal of Physical Chemistry B*, vol. 108, no. 45, pp. 17393–17397, 2004.

[11] S. F. Wuister, A. van Houselt, C. de Mello Donegá, D. Vanmaekelbergh, and A. Meijerink, "Temperature antiquenching of the luminescence from capped CdSe quantum dots." *Angewandte Chemie (International ed. in English)*, vol. 43, no. 23, pp. 3029–33, Jun. 2004.

[12] C. Carrillo-Carrión, S. Cárdenas, B. M. Simonet, and M. Valcárcel, "Quantum dots luminescence enhancement due to illumination with uv/vis light," *Chemical Communications*, no. 35, pp. 5214–5226, 2009.

[13] B. Luigjes, "Synthesis and optical properties of single and cross-linked quantum dots using mono- and dithiol-molecules," Master's thesis, Utrecht University, 2007.

[14] A. Franceschetti, A. Williamson, and A. Zunger, “Addition spectra of quantum dots: The role of dielectric mismatch,” *Journal of Physical Chemistry B*, vol. 104, no. 15, pp. 3398–3401, 2000.

[15] C. De Mello Donegá and R. Koole, “Size dependence of the spontaneous emission rate and absorption cross section of cdse and cdte quantum dots,” *Journal of Physical Chemistry C*, vol. 113, no. 16, pp. 6511–6520, 2009.

[16] C. de Mello Donegá, S. G. Hickey, S. F. Wuister, D. Vanmaekelbergh, and A. Meijerink, “Single-Step Synthesis to Control the Photoluminescence Quantum Yield and Size Dispersion of CdSe Nanocrystals,” *The Journal of Physical Chemistry B*, vol. 107, no. 2, pp. 489–496, Jan. 2003.

[17] W. Van Sark, P. Frederix, A. Bol, H. Gerritsen, and A. Meijerink, “EnglishBlueing, bleaching, and blinking of single cdse/zns quantum dots,” *EnglishChemPhysChem*, vol. 3, no. 10, pp. 871–879, 2002.

[18] A. Kahn, “EnglishThirty years of atomic and electronic structure determination of surfaces of tetrahedrally coordinated compound semiconductors,” *EnglishSurface Science*, vol. 299-300, no. C, pp. 469–486, 1994.

[19] D. D. Lovingood, R. Achey, A. K. Paravastu, and G. F. Strouse, “Size- and site-dependent reconstruction in CdSe QDs evidenced by 77Se{1H} CP-MAS NMR spectroscopy.” *Journal of the American Chemical Society*, vol. 132, no. 10, pp. 3344–54, Mar. 2010.

[20] C. Bullen and P. Mulvaney, “The effects of chemisorption on the luminescence of CdSe quantum dots.” *Langmuir*, vol. 22, no. 7, pp. 3007–13, Mar. 2006.

[21] I. Mekis, D. Talapin, A. Kornowski, M. Haase, and H. Weller, “One-pot synthesis of highly luminescent cdse/cds core-shell nanocrystals via organometallic and "greener" chemical approaches,” *Journal of Physical Chemistry B*, vol. 107, no. 30, pp. 7454–7462, 2003.

[22] C. Fang, M. a. van Huis, D. Vanmaekelbergh, and H. W. Zandbergen, “Energetics of polar and nonpolar facets of PbSe nanocrystals from theory and experiment.” *ACS nano*, vol. 4, no. 1, pp. 211–8, Jan. 2010.

[23] R. Koole, P. Schapotschnikow, C. de Mello Donegá, T. J. H. Vlugt, and A. Meijerink, “Time-dependent photoluminescence spectroscopy as a tool to measure the ligand exchange kinetics on a quantum dot surface,” *ACS Nano*, vol. 2, no. 8, pp. 1703–1714, 2008.

[24] B. Fritzinger, I. Moreels, P. Lommens, R. Koole, Z. Hens, and J. Martins, “EnglishIn situ observation of rapid ligand exchange in colloidal nanocrystal suspensions using transfer noe nuclear magnetic resonance spectroscopy,” *EnglishJournal of the American Chemical Society*, vol. 131, no. 8, pp. 3024–3032, 2009.

[25] A. Hassinen, I. Moreels, C. de Mello Donegá, J. C. Martins, and Z. Hens, “Nuclear Magnetic Resonance Spectroscopy Demonstrating Dynamic Stabilization of CdSe Quantum Dots by Alkylamines,” *Journal of Physical Chemistry Letters*, vol. 1, no. 17, pp. 2577–2581, Sep. 2010.

[26] R. L. Donkers, Y. Song, and R. W. Murray, “Substituent effects on the exchange dynamics of ligands on 1.6 nm diameter gold nanoparticles.” *Langmuir*, vol. 20, no. 11, pp. 4703–7, May 2004.

[27] G. a. Devries, M. Brunnbauer, Y. Hu, A. M. Jackson, B. Long, B. T. Neltner, O. Uzun, B. H. Wunsch, and F. Stellacci, "Divalent metal nanoparticles." *Science*, vol. 315, no. 5810, pp. 358–61, Jan. 2007.

[28] C. de Mello Donegá, M. Bode, and A. Meijerink, "Size- and temperature-dependence of exciton lifetimes in CdSe quantum dots," *Physical Review B*, vol. 74, no. 8, pp. 1–9, Aug. 2006.

[29] S. F. Wuister, C. de Mello Donegá, and A. Meijerink, "Luminescence temperature antiquenching of water-soluble CdTe quantum dots: role of the solvent." *Journal of the American Chemical Society*, vol. 126, no. 33, pp. 10397–402, Aug. 2004.

[30] C. B. Murray, D. J. Norris, and M. G. Bawendi, "Synthesis and characterization of nearly monodisperse cde (e = s, se, te) semiconductor nanocrystallites," *Journal of the American Chemical Society*, vol. 115, no. 19, pp. 8706–8715, 1993.

[31] D. V. Talapin, S. Haubold, A. L. Rogach, A. Kornowski, M. Haase, and H. Weller, "A novel organometallic synthesis of highly luminescent cdte nanocrystals," *Journal of Physical Chemistry B*, vol. 105, no. 12, pp. 2260–2263, 2001.

[32] S. F. Wuister, F. Van Driel, and A. Meijerink, "Luminescence and growth of cdte quantum dots and clusters," *Physical Chemistry Chemical Physics*, vol. 5, no. 6, pp. 1253–1258, 2003.

[33] C. de Mello Donegá, "Formation of nanoscale spatially indirect excitons: Evolution of the type-II optical character of CdTe/CdSe heteronanocrystals," *Physical Review B*, vol. 81, no. 16, pp. 1–20, Apr. 2010.

[34] N. Myung, Y. Bae, and A. Bard, "Enhancement of the photoluminescence of cdse nanocrystals dispersed in chcl3 by oxygen passivation of surface states,"*Nano Letters*, vol. 3, no. 6, pp. 747–749, 2003.

[35] M. Hines and P. Guyot-Sionnest, "Synthesis and characterization of strongly luminescing zns-capped cdse nanocrystals," *EnglishJournal of Physical Chemistry*, vol. 100, no. 2, pp. 468–471, 1996.

[36] B. C. Mei, J. Wang, Q. Qiu, T. Heckler, A. Petrou, and T. J. Mountziaris, "Dilution effects on the photoluminescence of ZnSe quantum-dot dispersions," *Applied Physics Letters*, vol. 93, no. 8, p. 083114, 2008.

[37] A. Komoto, S. Maenosono, and Y. Yamaguchi, "Oscillating fluorescence in an unstable colloidal dispersion of CdSe/ZnS core/shell quantum dots." *Langmuir*, vol. 20, no. 20, pp. 8916–23, Sep. 2004.

[38] J. K. Cooper, A. M. Franco, S. Gul, C. Corrado, and J. Z. Zhang, "Characterization of primary amine capped CdSe, ZnSe, and ZnS quantum dots by FT-IR: determination of surface bonding interaction and identification of selective desorption." *Langmuir*, vol. 27, no. 13, pp. 8486–93, Jul. 2011.

[39] W. K. Leung, K., "Surface relaxation in cdse nanocrystals," *Journal of Chemical Physics*, vol. 110, no. 22, pp. 11012–11022, 1999.

7 Appendices

Appendix A.1 shows an example of a fitted PL spectrum. Appendices A.2 to A.7 contain additional results that are not discussed in the main text.

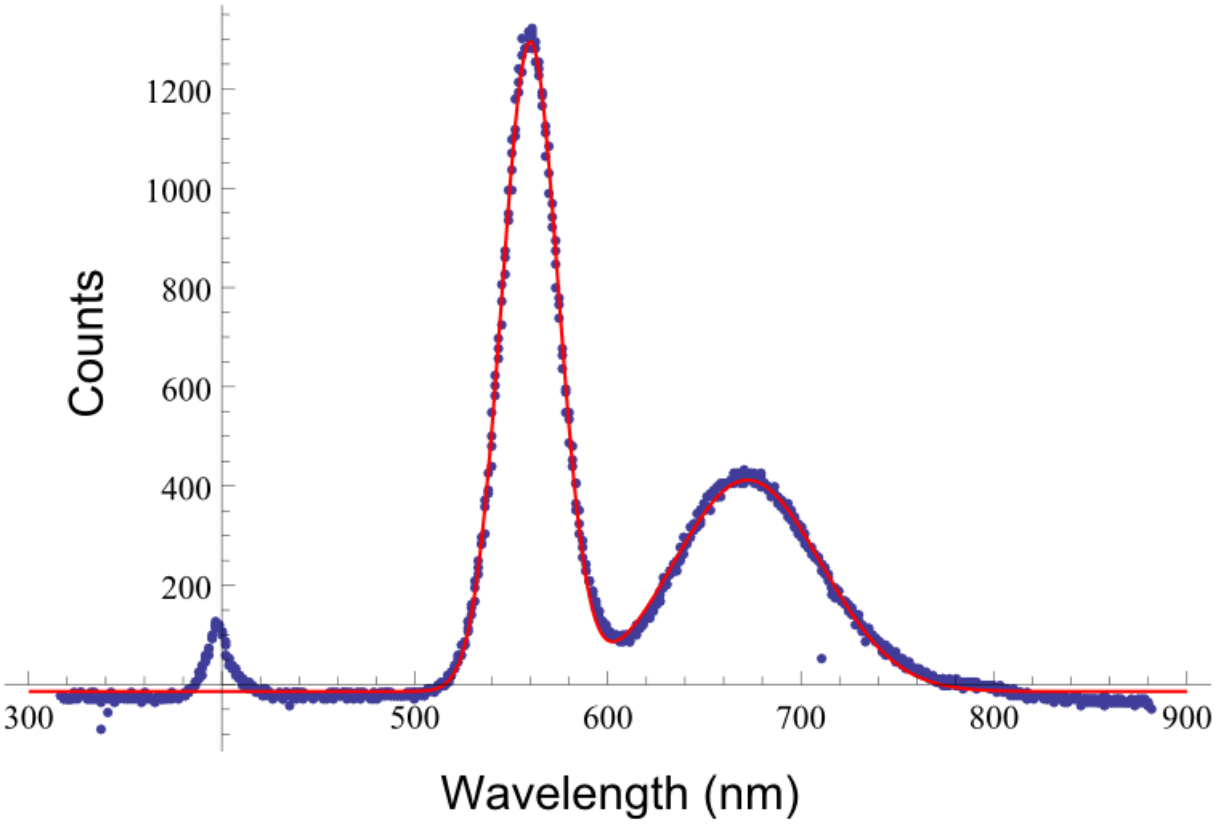

Figure A.1: *typical PL spectrum fitted with the sum of two Gaussian functions in Mathematica. Parameters from the fitted functions are used in the results discussed in paragraph 4.3. The minor peak at 400 nm is scattered excitation light and was ignored in the fits.*

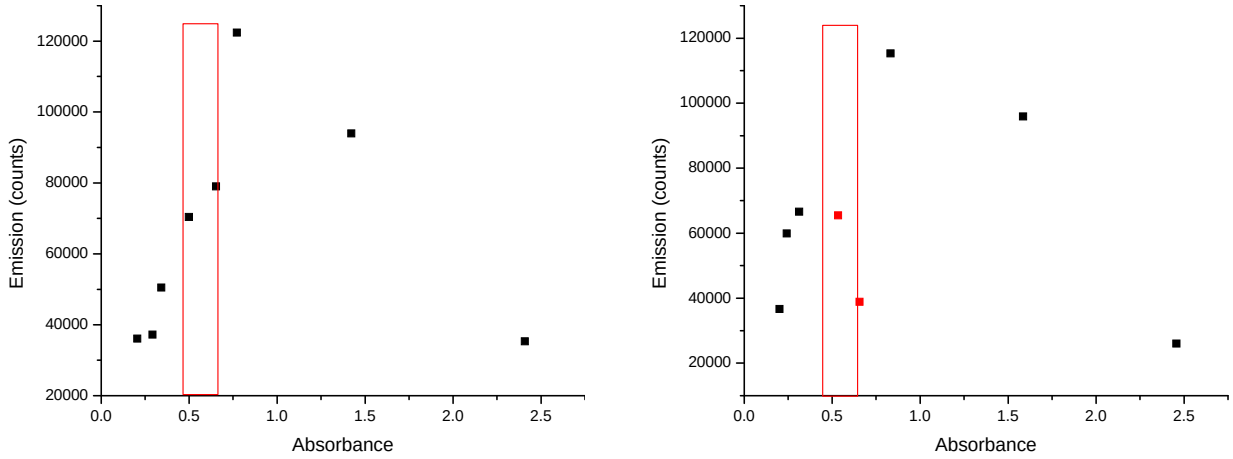

Figure A.2: *absorbance vs emission curves of dilutions in* ***(a)*** *2M DDA* ***(b)*** *toluene.*

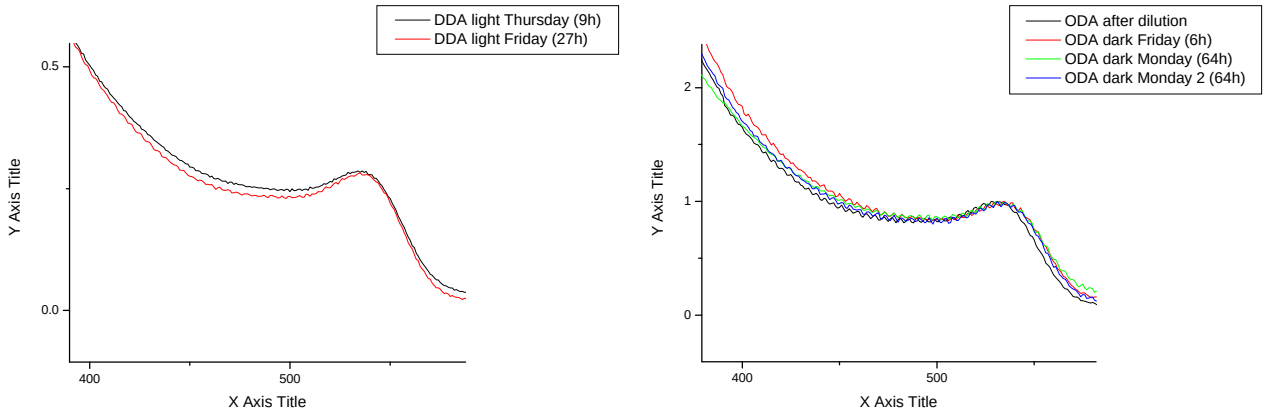

Figure A.3: *absorption spectra of* ***(a)*** *2M DDA* ***(b)*** *2M ODA samples*

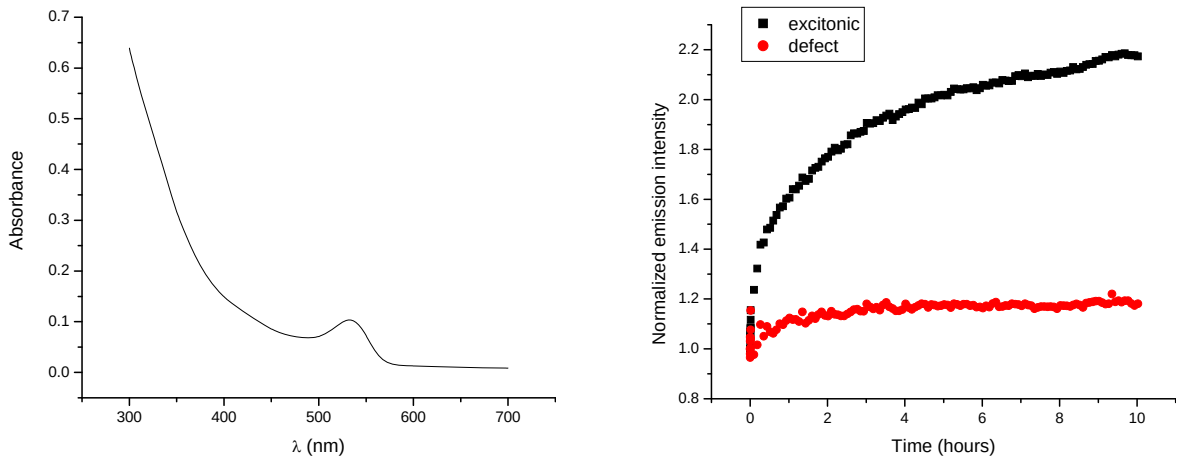

Figure A.4: ***(a)*** *absorption spectrum of FTIR sample, diluted 30x in dodecane. For the undiluted mixture [QD] = 15.7 uM, [DDA] = 1.1 M* ***(b)*** *PL series of a 100x dilution in dodecane*

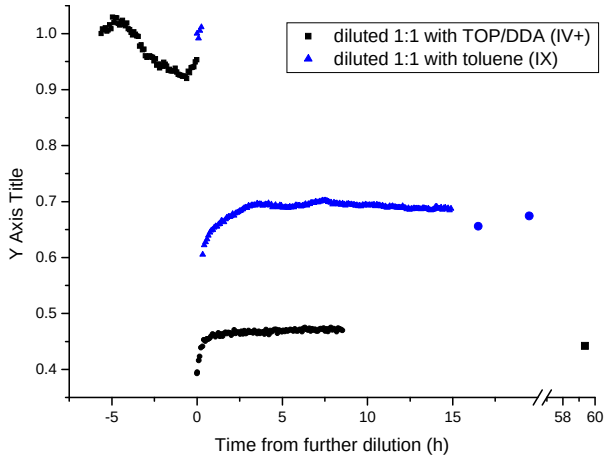

Sidenotes for this experiment:

- the excitation intensity is higher in the toluene dilution expriment

- the first LMSR trajectories of the two samples were similar but they were not from the same batch

Figure A.5: *when a sample that has already went through the LMSR is diluted again, it seems to evolve differently depending on whether it is diluted with toluene or ligands.*

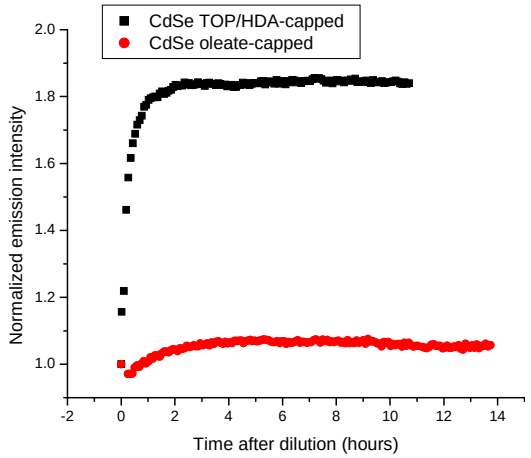

Figure A.6: *the LMSR effect in HDA-capped CdSe QDs.*

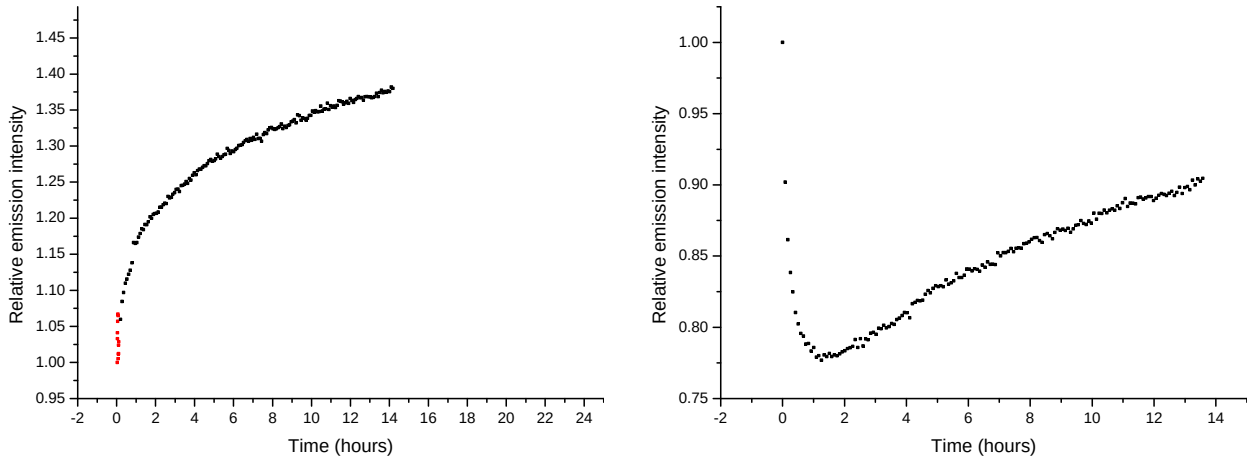

Figure A.7: *stirring seems to make no difference for the evolution. This makes sense because LMSR depends on diffusion of ligands, and diffusion speeds of ligands are high even without stirring.* ***(a)*** *freshly diluted, stirred* ***(b)*** *diluted 24 hours prior to measurement, stirred. The initial steep decrease in intensity seems to be an artifact.*